

**People's Democratic Republic of Algeria**  
**Ministry of Higher Education and Scientific Research**  
**University M'Hamed BOUGARA – Boumerdes**



**Institute of Electrical and Electronic Engineering**  
**Department of Electronics**

Final Year Project Report Presented in Partial Fulfilment of  
the Requirements for the Degree of

**MASTER**

**In Electrical and Electronic Engineering**  
**Option: Computer Engineering**

Title:

**Tissue Characterization of Brain using  
MRI**

Presented by:

- **BENTALEB Djouhra Lyza**
- **LARABI Farida**

Supervisor:

**Dr.D.Cherifi**

Registration Number:...../2016

## Dedication

---

### *Dedication*

*To my parents for their endless love, support and, encouragements*

*To my beloved father "Djilali" and my noble mother "Lila", who has successfully made me the person I am becoming. Thank you both for giving me strength to reach my dreams*

*To my dear little brother "Lounes", god bless him*

*To my supervisor Dr.D.Cherifi for her guidance and support throughout this work and especially for her confidence in me*

*To all my family, uncles, cousins, I cannot list all here, but you are always on my mind*

*To my beloved aunt "Sonia", you have always been there for me, your pray and advice were always helped me*

*To my precious cousin "Rachida", for her continuing long distance moral support, you are a sister for me, without forgetting her husband "Omar" and her little angel "Aylan"*

*To my dear grandmother "Hasni"*

*To the memory of my grandfathers "Mouhand Amokrane" and "Lounes", my grandmother "Djoher" who is the candle of my life, my uncle "Wahid" and his daughter "Celina" who is my inspiring model,*

*my god bless their soul*

*To all my friends, for their understanding in many moments of crisis, and especially the closest one*

*To all those with whom I spent wonderful moments in my life*

*I dedicate this modest work.*

# Acknowledgment

---

## **Acknowledgment**

First of all, we are highly appreciative of effort of our supervisor Dr.Cherifi Dalila for taking time to read through this report and her positive criticism of the project.

Sincere acknowledgment is given to our friend Boudjada.M who has provided us with data base and encouragement to improve the 3D algorithm.

We thank Dr.Hamadouche.A for sharing his medicine experiences, and knowledge.

Our appreciation goes to all IGEE staff for their guidance and helpful throughout this research.

Finally, we are deeply grateful to our parents for their efforts and concern while this work lasts.

## Dedication

---

*This work is humbly dedicated to the memory of my father the candle of my life, to my beloved mother. A special feeling of gratitude to my dear and only brother "Karim", my old sister "Nabila" the source of inspiration and her husband, my dear sister "Chabha" and her husband, my tender grandmother.*

*My nieces "Sarah", "Melina", "Melek", my nephew "Adem"*

*To all my friends specially my closest and beloved best friends Adel, Ayoub, Billal and Sofiane.*

*Farida*

# Abstract

---

## Abstract

In the evaluation of healthcare services, there is an increasing need for effective use of imaging data in medical diagnosis, the analysis and study of the brain is of great interest due to its potential for studying early growth tumor which is an abnormal mass of tissue found in the brain.

The purpose of the project is to characterize an abnormal tissue of brain MRI Imaging, especially the brain tumor. For that, we have firstly used different methods of segmentation which are thresholding, K-means and fuzzy K-means in order to extract the tumor, secondly 3D reconstruction of the tumor has been involved by applying the pre-processing and post-processing steps to get the better image's results which are inputted as a 2D parallel slices in the marching cube algorithm to form a 3D tumor's volume. After that the texture analysis is presented as a useful computational method for discriminating between pathologically different regions on medical images because it has been proven to perform better than human eyesight at discriminating certain classes of texture. Finally, an experimental part has been done on where the results of the extraction's segmentation and texture analysis are discussed, in addition 3D reconstruction is implemented.

# Table of Content

---

Acknowledgements.....	I
Dedication .....	II
Abstract.....	IV
Table of Contents.....	V
List of Figures.....	VIII
List of tables.....	IX
General Introduction.....	1
Chapter I Medical Imaging using MRI.....	2
I.1. Introduction.....	3
I.2. Brain description .....	3
I.3. Brain Tumors .....	4
I.3.1. Brain tumor symptoms.....	4
I.4. MR Image Characteristics.....	4
I.4.1. Structure of the MRI Scanner.....	5
I.4.2. The difference between MRI and CT scan's methods.....	6
I.4.3. Benefits of an MRI scans.....	6
I.5. Summary.....	7
Chapter II Tumor Extraction and 3D Reconstruction.....	8
II.1. Introduction.....	9
II.2. Threshold Algorithm.....	9
II.3. Threshold detection methods .....	9
II.3.1. Global (Fixed) thresholding.....	9
II.3.2. Local (or dynamic) thresholding.....	10
II.3.3. The Otsu method (Optimal thresholding).....	10
II.3.3.1. Iterative optimal threshold selection.....	10
II.3.3.2. Faster Approach of Otsu method.....	12
A. Between/Within/Total Variance.....	12
II.4. Advantages and Disadvantages of Threshold Algorithm.....	12
a. Advantages .....	12
b. Disadvantages .....	12

# Table of Content

---

II.5. K-means Clustering Algorithm.....	13
II.6. Fuzzy K-means.....	14
II.6.1. Fuzzy K-means Algorithm.....	15
a. Algorithmic steps for Fuzzy K-means clustering.....	15
b. Remarks.....	16
c. Advantages.....	16
d. Disadvantages.....	16
II.7. post-processing Step.....	17
II.8. 3D Reconstruction using Marching Cube Algorithm.....	17
II.9. Proposed Methodology.....	18
II.9.1. Pre processing of different slices.....	19
II.9.2. Extraction of tumor in different slices.....	20
II.9.3. Slice Interpolation.....	20
II.9.4. Mesh generation using Marching cubes.....	20
II.9.5. Rendering.....	22
II.10. Summary.....	23
Chapter III .Texture analysis.....	24
III.1. Introduction.....	25
III.2 Texture analysis.....	25
III.2.1 First-Order Statistical Texture Analysis.....	25
III.2.2 Second-Order Statistical Texture Analysis.....	26
III.2.2.1 The grey Level Co-occurrence Matrix.....	27
III.3. GLCM parameters.....	27
III.3.1 Contrast.....	27
III.3.2 Correlation.....	27
III.3.3 Energy.....	28
III.3.4 Homogeneity.....	28
III.3.5 Entropy.....	28

# Table of Content

---

III.3.6 Mean.....	28
III.3.7 Variance.....	28
III.4 Summary.....	29
Chapter IV. Results and Discussion.....	30
IV.1 Comparative study of segmentation method on brain tumor's extraction.....	31
IV.1.1 Thresholding processing.....	31
IV.1.2 K-Means processing.....	33
IV.2 Marching Cube algorithm Results.....	35
IV.3 Texture analysis procedure.....	42
IV.4 Summary.....	52
Conclusion.....	53

## List of Figures

---

<b>Figure I.1:</b> Brain's planes.....	3
<b>Figure I.2:</b> MR Image of the brain .....	5
<b>Figure I.3:</b> MRI Equipment.....	5
<b>Figure II.1:</b> Segmented MRI Image for threshold algorithm.....	13
<b>Figure II.2:</b> Segmented MRI Image for K-means algorithm.....	14
<b>Figure II.3:</b> Example of Fuzzy K-means clustering.....	16
<b>Figure II.4:</b> Flowchart of the Proposed 3D Tumor Reconstruction Approach .....	19
<b>Figure II.5:</b> Triangulated Cubes.....	21
<b>Figure II.6:</b> Cube Numbering.....	22
<b>Figure III.1:</b> Example of GLCM showing the different direction of $\theta$ .....	26
<b>Figure IV.1:</b> Results of improved Threshold Algorithm for tumor extraction.....	33
<b>Figure IV.2:</b> The four samples used in the texture analysis.....	42
<b>Figure IV.3:</b> Contrast values for different samples (bone, grey matter, tumor, csf) with $\theta=0^\circ$ .....	43
<b>Figure IV.4:</b> Contrast values for different samples (bone, grey matter, tumor, csf) with $\theta=45^\circ$ .....	43
<b>Figure IV.5:</b> Contrast values for different samples (bone, grey matter, tumor, csf) with $\theta=90^\circ$ .....	44
<b>Figure IV.6:</b> Contrast values for different samples (bone, grey matter, tumor, csf) with $\theta=135^\circ$ .....	44
<b>Figure IV.7:</b> Homogeneity values for different samples (bone, grey matter, tumor, csf) with $\theta=0^\circ$ .....	45
<b>Figure IV.8:</b> Homogeneity values for different samples (bone, grey matter, tumor, csf) with $\theta=45^\circ$ .....	45
<b>Figure IV.9:</b> Homogeneity values for different samples (bone, grey matter, tumor, csf) with $\theta=90^\circ$ .....	46
<b>Figure IV.10:</b> Homogeneity values for different samples (bone, grey matter, tumor, csf) with $\theta=135^\circ$ .....	46
<b>Figure IV.11:</b> Correlation values for different samples (Bone, GreyMatter, Tumor, CSF) with $\theta=0^\circ$ .....	47
<b>Figure IV.12:</b> Correlation values for different samples (bone, gray matter, tumor, csf) with $\theta=45^\circ$ .....	47
<b>Figure IV.13:</b> Correlation values for different samples (bone, gray matter, tumor, csf) with $\theta=90^\circ$ .....	48
<b>Figure IV.14:</b> Correlation values for different samples (bone, gray matter, tumor, csf) with $\theta=135^\circ$ .....	48
<b>Figure IV.15:</b> Energy values for different samples (bone, gray matter, tumor, csf) with $\theta=0^\circ$ .....	49
<b>Figure IV.16:</b> Energy values for different samples (bone, gray matter, tumor, csf) with $\theta=45^\circ$ .....	49
<b>Figure IV.17:</b> Energy values for different samples (bone, gray matter, tumor, csf) with $\theta=90^\circ$ .....	50
<b>Figure IV.18:</b> Energy values for different samples (bone, gray matter, tumor, csf) with $\theta=135^\circ$ .....	50
<b>Figure IV.19:</b> The mean for different samples (bone, gray matter, tumor, csf) with $\theta=0^\circ$ .....	51
<b>Figure IV.20:</b> The mean for different samples (bone, gray matter, tumor, csf) with $\theta=45^\circ$ .....	51
<b>Figure IV.21:</b> The mean for different samples (bone, gray matter, tumor, csf) with $\theta=90^\circ$ .....	52
<b>Figure IV.22:</b> The mean for different samples (bone, gray matter, tumor, csf) with $\theta=135^\circ$ .....	52

## List of tables

---

<b>Table IV.1:</b> Results of Threshold Algorithm for tumor extraction.....	31
<b>Table IV.2:</b> Results of Threshold Algorithm for tumor extraction with mistakes.....	32
<b>Table IV.3:</b> Results of K-Means Algorithm for tumor extraction.....	34
<b>Table VI.4:</b> Results of the steps used for tumor extraction.....	40
<b>Table IV.5:</b> 3D Reconstruction using marching cube.....	41

## Introduction

Brain tumors are inherently serious and life-threatening because of its invasive and infiltrative character in the limited space of the intracranial cavity. In medical treatment of tumor patients magnetic resonance imaging (MRI) systems are of increasing importance in diagnosis, and supervision. In particular when facing brain tumors exact knowledge about the localization and extension of the tumor in the skull is essential for surgical procedures as well as for radiotherapy. MRI uses radio waves and magnetic fields to acquire a set of cross sectional images of the brain. That is anatomic details of the 3D tumor are presented as a set of 2D parallel cross sectional images. The standard process of human interpretation and diagnosis of these images is based on the expert knowledge of the physician and on the significant differences of tissue textures in the images. Usually, affected areas are indicated by interactive editing of the image. For these reasons, an automatic procedure as a support for the interpretation, classification and fast 3D-reconstruction of the initial images would be very helpful to the physician.

In surgery, the tumor has to be removed entirely without damaging other important parts of the brain, nerves or veins.

This work will describe an application of the methods introduced for the visualization and interpretation of brain tumors from MR images. It will show how these methods work and how they can successfully separate tissue types. For reasons of performance in clinical procedures, we use a modified marching cubes algorithm for fast 3D-reconstruction.

The work will be organized in four main chapters:

- The first chapter introduces the basic understanding concepts of brain MRI technique.
- The second chapter is divided into two sections which are: tumor extraction and its 3D reconstruction.
- The third chapter talks about the texture analysis where several parameters from the GLCM matrix will be presented to characterize different texture regions.
- The fourth chapter consists of the results and discussion of tumor extraction, 3D reconstruction and texture analysis.

# Chapter I

## Medical Imaging using MRI

### MRI

- MRI stands for Magnetic Resonance Imaging.
- Magnetic resonance imaging (**MRI**) is a technique that uses a magnetic field and radio waves to create detailed images of the organs and tissues within your body.



---

By the increasing use of direct digital imaging systems for medical diagnostics, digital image processing becomes more and more important in health care, digital methods, such as Computed Tomography (CT) or Magnetic Resonance Imaging (MRI) are used for abnormal tissues detection. In this chapter, we will introduce the background knowledge of brain tumor in MR images and MR image characteristics.

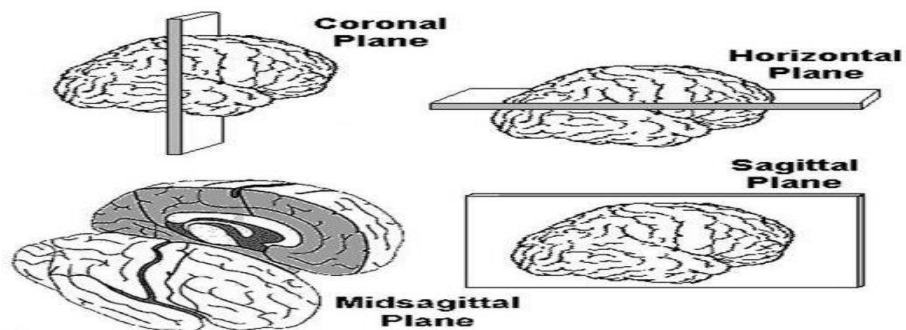
---

## I.1. Introduction

Medical imaging refers to several different technologies that are used to view the human body in order to diagnose, monitor, or treat medical conditions. Each type of technology gives different information about the area of the body being studied or treated, related to possible disease, injury, or the effectiveness of medical treatments. In this chapter we are going to discuss different types of these medical images, the tools used to get them and some of medical cases.

## I.2. Brain description

The brain is one of the largest and most complex organs in the human body. It is made up of more than 100 billion nerves that communicate in trillions of connections called synapses. It controls our muscle movements, internal temperature, and even our breathing and every creative thought, feeling, and plan is developed by our brain. This last, like all biological structures, is three dimensional which means that any point inside the brain can be localized on three "axis" or "planes" - the x, y and z axis. The brain is often imaged on two-dimensional images (slices). These slices are usually made in one of three orthogonal planes: coronal, horizontal (axial) and sagittal. Figure. I.1 shows these sections.



**Figure I.1:** Brain's planes

### **I.3. Brain Tumors**

Tumors are abnormal masses caused by the abnormal growth of body cells that occupies unnecessary space in the body. Generally, brain tumors are of two types: benign and malignant. A benign tumor does not spread in a rapid manner and does not affect healthy neighboring cells. These tumor cells, instead of spreading throughout the whole body, grow in a limited space and form a lump, nodules and moles are examples of benign tumors. Malignant tumors such as glioblastoma multiform (GBM made of glial tissue, make up more than 50% of all brain tumors) conversely, spread throughout the body with time, affecting all organs, and ultimately result in the death of the patient. A brain tumor can be classified based on:

- i) where the tumor is located
- ii) The type of tissues involved
- iii) Whether it is benign or malignant.

The primary cause of brain tumors is unknown. However environmental and genetic factors may play a role or priori exposure to therapeutic irradiation.

#### **I.3.1. Brain tumor symptoms**

Brain tumor symptoms include headaches, nausea, seizures, behavior changes, memory loss, vision and hearing problems. For this reason many treatment options are available on different criteria, which depend on the size and the type of tumor, growth rate and general health of the patient. These treatments generally include radiation therapy, chemotherapy and surgery.

### **I.4. MR Image Characteristics**

Magnetic Resonance Imaging (MRI) is an imaging modality used in radiology for diagnostic purposes. It is a technique that uses nuclear magnetic resonance to form cross sectional images and gives information about the complex anatomic structures of the human body. These complex 3D anatomic structures are presented as 2D images.

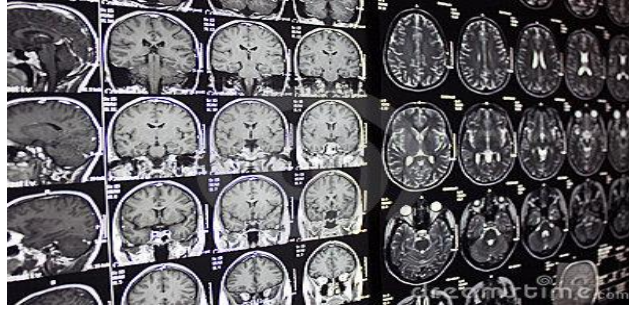


Figure I.2: MR Image of the brain

### I.4.1. Structure of the MRI Scanner

The scanner is of tabular shaped, it's around 60cm in diameter, and if the diameter is too wide, the magnetic force might not be strong enough.

The Magnetic Resonance Imaging is structured as follows:

- **Magnet:** The biggest and the most important part in an MRI scanner .It consists of many coils of wire through which electricity passes, resulting in a huge magnetic field.
- **Set of coils:** They are used for transmitting radio frequency waves for different parts of the body.
- **Radio Frequency coil, Scanner and patient table .**

The figure |I.3| illustrates the above structure.

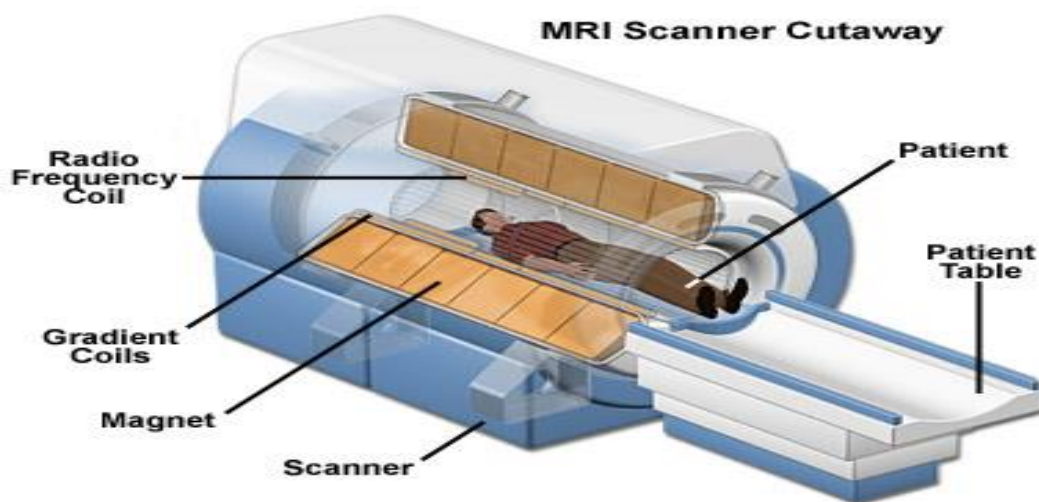


Figure I.3: MRI Equipment

## **I.4.2. The difference between MRI and CT (Computed Tomography) scan's methods**

The development of tumors in the brain can be diagnosed with both CT and MRI scans, but only MRI has the resolution to detect heterogeneity within tumors that might indicate its origin.

MRI is more sensitive for brain tumors than CT (Computed Tomography), that scans use x-ray radiation for scanning, which is harmful to the human brain, whereas MRIs use strong magnetic field and radio waves that generate a high quality scan as opposed to CT both in terms of detection as well as in showing more completely the extent of the tumor. MRI provides significantly more information about intrinsic tissue characterization and parallels findings on gross pathology. MRI uniquely depicts hemorrhage, because of the paramagnetic properties of many of the blood-breakdown products. The signal intensity pattern of intratumoral hemorrhage differs from benign intracranial hematomas. Fat-containing neoplasms (e.g., teratoma, dermoid, lipoma) are easily identified on MRI. The dilated and increased blood vessels to the tumors may also be seen well on MRI and magnetic resonance angiography (MRA).

## **I.4.3. Benefits of an MRI scans**

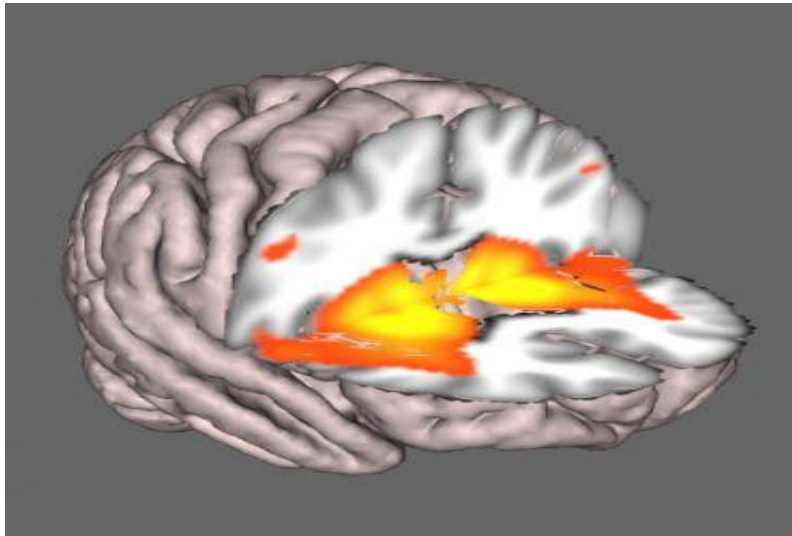
MRI scans are an important tool that doctors use to investigate the cause of symptoms. They can confirm the presence or absence of a disease or injury. However, the diagnosis requires more than a single examination or test. An MRI scan should always be used to supplement doctor's examination. Some properties of MRI are:

- Provide very detailed diagnostic pictures of most of the important organs and tissues in your body
- Are generally painless
- Are sometimes able to show unique information that other tests are unable to show
- Do not use radiation and are therefore suitable for use for children and pregnant women.

## **I.5. Summary**

In this chapter, we started by introducing the medical imaging, then we gave a brief description of the brain and some brain tumor generalities and symptoms after that we discussed about different characteristics of the magnetic resonance imaging and the structure of the MRI scanner then we talked about the difference between MRI and CT's scan at the end we showed some of the benefits of the MRI.

## Chapter II



## Tumor Extraction and 3D Reconstruction

---

Understanding images and extracting the information from them such that the information can be used for other tasks is an important aspect of Machine learning. Like extracting malign tissues from body scans form integral part of Medical diagnosis. One of the first steps in direction of understanding images is to segment them and find out different objects in them. To do this, features like the histogram plots and the frequency domain transform can be used. Image segmentation is one of the mostly used methods to classify the pixels of an image correctly in a decision oriented application. It divides an image into a number of discrete regions such that the pixels have high similarity in each region and high contrast between regions.

In this chapter, we define different methods namely **thresholding algorithm**, **K Means clustering**, **fuzzy K-means** and **post-processing step** for image segmentation which will be used in 3D reconstruction of the tumor using the marching cube algorithm.

---

## II.1. Introduction

Medical images are segmented using different techniques and process outputs are used for the further analysis in medical. One of the fundamental problems in medical analysis is the image segmentation which identifies the boundaries of objects such as organs or abnormal region in images. There are two types of segmentations: soft segmentations and hard segmentations; Segmentations that allow regions or classes to overlap are called soft segmentations whereas a hard segmentation forces a decision of whether a pixel is inside or outside the object [1]. Results from the segmentation make it possible for shape analysis, detecting volume change, and making a precise radiation therapy treatment plant. Brain tumor extraction is the aim of this chapter, to make it possible we used different segmentation methods such as: **Threshold algorithm**, **K-means clustering** and **Fuzzy C-means clustering**.

## II.2. Threshold Algorithms

Segmentation involves separating an image into regions (or their contours) corresponding to objects. We usually try to segment regions by identifying common properties, or similarly, we identify contours by identifying **differences** between regions (edges). The simplest property that pixels in a region can share is intensity. So, a natural way to segment such regions is through **thresholding**, the separation of light and dark regions. Thresholding creates binary images from grey-level ones by turning all pixels below some threshold to zero and all pixels about that threshold to one.

## II.3. Threshold detection methods

Different methods for choosing a threshold can be used. Automatically selected threshold value for each image by the system without human intervention is called **an automatic threshold scheme**(ex: Optimal thresholding).This require the knowledge about the intensity characteristics of the objects, sizes,fractions of the image occupied by the objects and the number of different types of objects appearing in the image. Users can also choose **manually** a threshold value.

### II.3.1. Global (Fixed) thresholding

According to this method, all pixels are compared to a same value in the thresholding procedure. This value may be constant, or be chosen from image histogram:

$$g(X, Y) = \begin{cases} 0 & \text{if } F(X, Y) < T \\ 1 & \text{if } F(X, Y) \geq T \end{cases} \quad (\text{II.1})$$

### II.3.2. Local (or dynamic) thresholding

The image is divided into overlapping sections which are thresholded one by one, it depends on the position in the image. Unlike global thresholding method, this approach compute an independent threshold for each pixel over a local window whose center is the pixel being binarizing.

### II.3.3. The Otsu method (Optimal thresholding)

Otsu's thresholding method involves iterating through all the possible threshold values and calculating a measure of spread for the pixel levels for each side of the threshold, i.e. the pixels that either fall in foreground or background.

The aim is to find the threshold value where the sum of foreground and background spreads is at its minimum.

- Optimal thresholding methods select the threshold based on the minimization of a criterion function.
- The criterion for Otsu is the minimization of **the within-group variance** of the two groups of pixels separated by the threshold.

#### II.3.3.1. Iterative optimal threshold selection

The Simplest case is the segmentation into two classes, so the intensities in each class will be our clusters and we want to find a threshold such that each pixel on each side of the threshold is closer in intensity to the mean of all pixels on that side of the threshold than to the mean of all pixels on the other side of the threshold. So, for each potential threshold **T** we have to:

1. Select an initial estimate for **T**
2. Segment the image using **T**; separate the pixels into two clusters according to the threshold, this produces **2** groups: **G1** pixels with **value**  $\geq T$  and **G2** with **value**  $< T$ .
3. Compute the mean of each cluster  **$\mu_1$**  and  **$\mu_2$** , average pixel values of **G1** and **G2**
4. Square the difference between the means.
5. Multiply by the number of pixels in one cluster times the number in the other.
6. Repeat steps **2** to **5** until **T** stabilizes.

The calculations for finding **the foreground and background variances** (the measure of spread) for a single threshold are now shown. Then **the class probabilities** are estimated as:

Let group O (Foreground) be those pixels with greylevel  $< T$

Let group B (Background) be those pixels with greylevel  $\geq T$

$$P_o(T) = \frac{1}{N} \sum_{i=0}^{T-1} h(i) \quad (\text{II.2})$$

$$P_b(T) = \frac{1}{N} \sum_{i=T}^{L-1} h(i) \quad (\text{II.3})$$

Where  $h(i)$  is the histogram of an N pixel image,  $P_o(T)$  is the prior probability of group **O** and  $P_b(T)$  is the prior probability of **B**.

And **the class means** are given by:

$$\mu_o = \frac{1}{N_o} \sum_{i=0}^{T-1} i \cdot h(i) \quad (\text{II.4})$$

$$N = N_o + N_b$$

$$\mu_b = \frac{1}{N_b} \sum_{i=T}^{L-1} i \cdot h(i) \quad (\text{II.5})$$

Finally, **the individual class variances** are:

$$\sigma_o^2 = \frac{1}{N_o} \sum_{i=0}^{T-1} (i - \mu_o)^2 \cdot h(i) \quad (\text{II.6})$$

$$\sigma_b^2 = \frac{1}{N_b} \sum_{i=T}^{L-1} (i - \mu_b)^2 \cdot h(i) \quad (\text{II.7})$$

The next step is to calculate the '**Within-Class Variance**'. This is simply the sum of the two variances multiplied by their associated probabilities (weights).

**The weighted within-class variance** is:

$$\sigma_w^2(T) = \sigma_b^2(T)P_b(T) + \sigma_o^2(T)P_o(T) \quad (\text{II.8})$$

This final value is the '**sum of weighted variances**' for the given threshold value. The same calculation needed to be performed for all the possible threshold values **0 to (L-1)**. (L is the grayscale level) and **pick the value that minimizes  $\sigma_w^2(T)$** . This approach for calculating Otsu's threshold is useful for explaining the theory, but it is computationally intensive, especially if you have a full **8-bit** greyscale. The next section shows a faster method of performing the calculations which is much more appropriate for implementations.

### II.3.3.2. Faster Approach of Otsu method

By a bit of manipulation, we can calculate what is called the **between class** Variance which is far quicker to calculate. Luckily, the threshold with the maximum **between class** variance also has the minimum **within class** variance. So it can also be used for finding the best threshold and therefore due to being simpler is a much better approach to use.

#### A. Between/Within/Total Variance

The basic idea is that the total variance does not depend on threshold (obviously). For any given threshold, the total variance is the sum of the **within-class** variances (weighted) and the **between-class** variance, which is the sum of weighted squared distances between the class means and the grand mean.

Within Class Variance as given by (Eq II.8):

$$\sigma_w^2(T) = \sigma_b^2(T)P_b(T) + \sigma_o^2(T)P_o(T)$$

Between Class Variance:

$$\begin{aligned}\sigma_B^2(T) &= \sigma^2(T) - \sigma_w^2(T) \\ &= P_b(\mu_b - \mu)^2 + P_o(\mu_o - \mu)^2 \\ &= P_bP_o(\mu_b - \mu_o)^2\end{aligned}\tag{II.9}$$

where ( $\mu = P_b\mu_b + P_o\mu_o$ )

After some algebra, we can express the total variance as:

$$\sigma^2 = \sigma_w^2(T) + \sigma_b^2(T)\tag{II.10}$$

Since the total is constant and independent of  $\mathbf{T}$ , the effect of changing the threshold is merely to move the contributions of the two terms back and forth.

So, **minimizing the within-class** variance is **the same as maximizing the between-class** variance. Operates directly on the gray level histogram [e.g. 256 numbers,  $P(i)$ ], so it's fast (once the histogram is computed).

## II.4. Advantages and Disadvantages of Threshold Algorithm

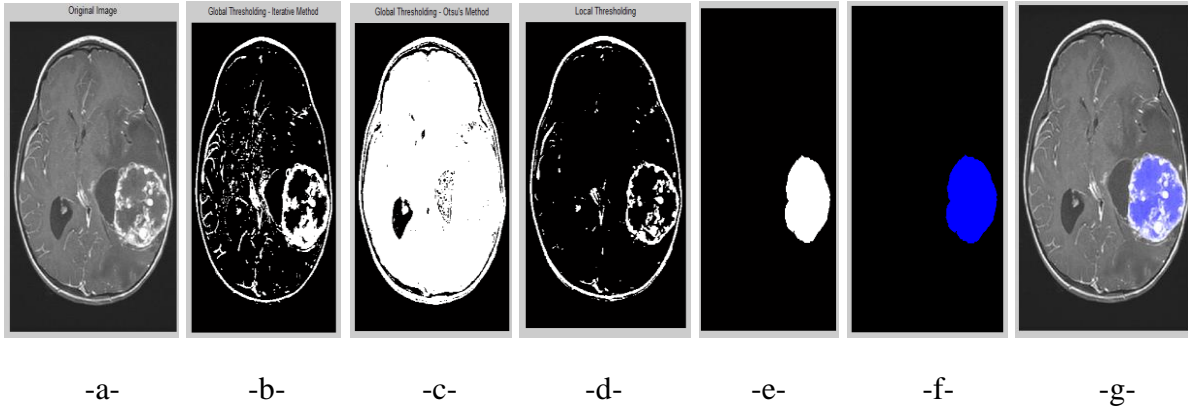
### a. Advantages

- Simple to implement.
- Faster.
- Good for some kinds of images (e.g: documents, controlled lighting).

### b. Disadvantages

- No guarantees of object coherency; may have holes, extraneous pixels.
- Incomplete solution: post-processing with morphological operators.

The figure bellow shows the results of different methods for detecting the tumor as the global thresholding (Iterative and Otsu method), local thresholding.



**Figure II.1:** Segmented MRI Image for threshold algorithm a) Original GBM tumor image, b) Global thresholding –Iterative method-c) Global thresholding –Otsu method- d) Local thresholding e) Dilated grey scale image f) Result of (e) overlaid g) Tumor overlaid on the original image.

## II.5. K-means Clustering Algorithm

K-Means algorithm is simple and computationally faster than the hierarchical clustering, furthermore it works for large number of variables, but it produces different cluster results for different number of cluster. As a result it is required to initialize the proper number of cluster, as well as the initialization of the  $k$  number of centroid. Different value of initial centroid would result in different cluster. Moreover selection of proper initial centroid is also an important task. K-means is an unsupervised clustering algorithm that classifies the input data points into multiple classes based on their inherent distance from each others, this algorithm assumes that the data features form a vector space and tries to find natural clustering in them, the points are clustered around centroids  $\mu_i \forall i = 1 \dots k$  which are obtained by minimizing the objective

$$V = \sum_{i=1}^k \sum_{x_j \in S_i} (x_j - \mu_i)^2 \quad (\text{II.11})$$

Where there are  $k$  clusters  $S_i, i = 1, 2, \dots, k$  and  $\mu_i$  is the centroid or mean point of all the points  $x_j \in S_i$

As a part of this project, an iterative version of the algorithm was implemented, which takes a 2 dimensional image as input. The steps of the algorithm are as follows:

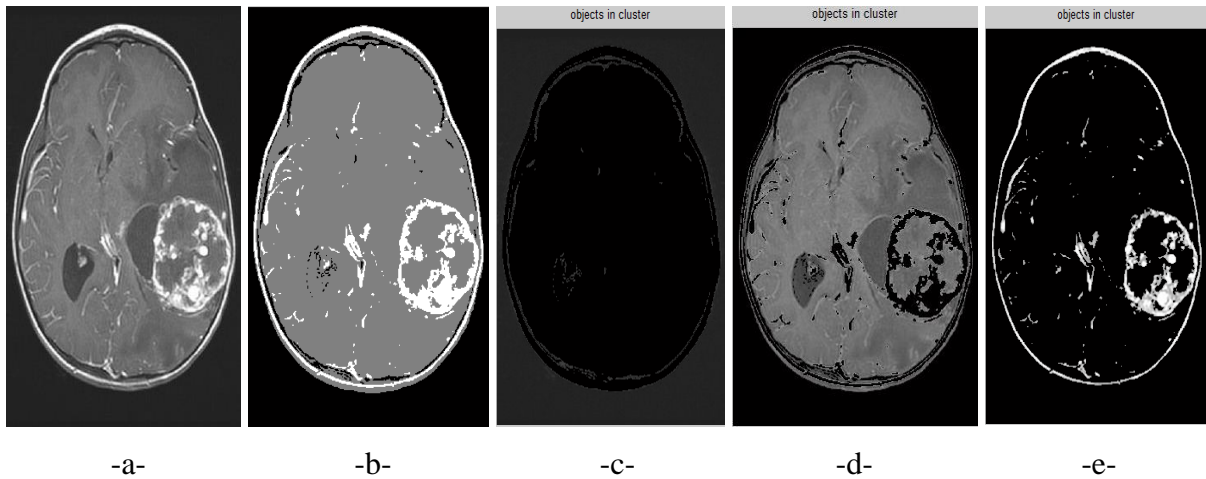
- 1) Compute the intensity distribution (also called the histogram) of the intensities.
- 2) Initialize the centroids with k random intensities.
- 3) Repeat the following steps until the cluster labels of the image do not change anymore.
- 4) Cluster the points based on distance of their intensities from the centroid intensities.

$$C^{(i)} = \mathit{arg\ min}_j \|x^{(i)} - \mu_j\|^2 \quad (\text{II.12})$$

- 5) Compute the new centroid for each of the clusters.

$$\mu_i = \frac{\sum_{j:N_i} x_j}{N_i}, i=1, \dots, k \quad (\text{II.13})$$

By applying the K-means algorithm to an MRI image the results are shown in the figure below:



**Figure II.2:** Segmented MRI Image for K-means algorithm a) Original GBM tumor image  
b) Result of (a) on Gray scale, c) Object in cluster1 d) Object in cluster2 e) Object in cluster3

## II.6. Fuzzy K-means

Fuzzy K-means is an extension to the standard K-means algorithm by introducing a penalty term to the objective function to make the clustering process not sensitive to the initial cluster centers. The new algorithm can produce more consistent clustering results from different sets of initial clusters centers. Combined with cluster validation techniques, the new algorithm can determine the number of clusters in a data set, which is a well known problem in k-means clustering.

Fuzzy K-means or Fuzzy c-mean (FCM) is one of the most used methods of clustering for image segmentation which allows one piece of data to belong to two or more clusters, and its success chiefly attributes to the introduction of fuzziness for the belongingness of each

image pixels. Compared with crisp or hard segmentation methods, FCM is able to retain more information from the original image. However, one disadvantage of standard FCM is not to consider any spatial information in image context, which makes it very sensitive to noise and other imaging artifacts. This method was developed by Dunn in 1973 and improved by Bezdek in 1981 and it is frequently used in pattern recognition.

### II.6.1. Fuzzy K-means Algorithm

The algorithm is based on minimization of the following objective function:

$$J_m = \sum_{i=1}^N \sum_{j=1}^C \mu_{ij}^m \|x_i - C_j\|^2, \quad 1 \leq m < \infty \quad (\text{II.14})$$

Where  $m$  is any real number greater than 1,  $\mu_{ij}$  is the degree of membership of  $x_i$  in the cluster  $j$ ,  $x_i$  is the  $i^{\text{th}}$  of  $d$ -dimensional measured data,  $C_j$  is the  $d$ -dimension center of the cluster, and  $\|*\|$  is any norm expressing the similarity between any measured data and the center.

#### a. Algorithmic steps for Fuzzy K-means clustering

We use an algorithm to determine all the centroids. (For example: arithmetic means of all data points) and we run FCM several times each starting with different initial centroids. The steps of this algorithm are summarized as follows:

**Step 1:** Initialize  $U = [\mu_{ij}]$  matrix,  $U(0)$

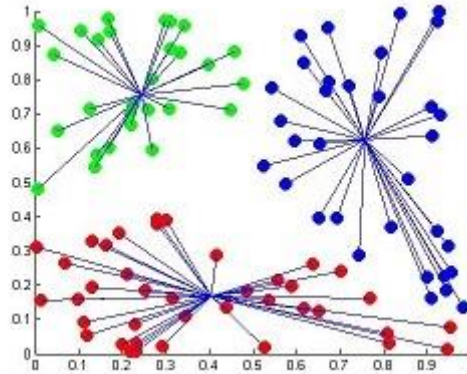
**Step 2:** At  $k$ -step: calculate the centers vectors  $C(k) = [C_j]$  with  $U(k)$

$$C_j = \frac{\sum_{i=1}^N \mu_{ij}^m x_i}{\sum_{i=1}^N \mu_{ij}^m} \quad (\text{II.15})$$

**Step 3:** Update  $U(k)$ ,  $U(k+1)$

$$\mu_{ij} = \frac{1}{\sum_{k=1}^C \left( \frac{\|x_i - C_j\|}{\|x_i - C_k\|} \right)^{\frac{2}{m-1}}} \quad (\text{II.16})$$

**Step 4:** If  $\|U(k+1) - U(k)\| < \text{threshold } \varepsilon$  then STOP; otherwise return to step 2.



**Figure II.3:** Example of Fuzzy K-means clustering

### b. Remarks

- The computation of the updated membership function is the condition for the minimization of the objective function.
- With fuzzy  $k$ -means, the centroid of a cluster is computed as being the mean of all points, weighted by their degree of belonging to the cluster.
- The degree of being in a certain cluster is related to the inverse of the distance to the cluster.
- By iteratively updating the cluster centers and the membership grades for each data point, FCM iteratively moves the cluster centers to the "right" location within a data set.
- Performance depends on initial centroids. For a robust approach there are two ways which is described below.

### c. Advantages

- Gives best result for overlapped data set and comparatively better than K-means algorithm.
- Unlike  $k$ -means where data point must exclusively belong to one cluster center here data point is assigned membership to each cluster center as a result of which data point may belong to more than one cluster center.

### d. Disadvantages

- Apriori specification of the number of clusters.
- With lower value of  $\beta$  we get the better result but at the expense of more number of iteration.

- Euclidean distance measures can unequally weight underlying factors.

## II.7. post-processing Step

The following computational step has to apply for image segmentation process on the image taken as input to get the required segmented data after pre-processing and image segmentation. Post-processing of CT and MRI images has been increasing due to a large increase in clinical demand, becoming indispensable in daily practice. It has proven to be a valuable tool in a variety of clinical applications due to its ability to provide additional diagnostic information. It has applications in various organs and systems such as neuroradiology and cardiovascular. It is essential to have image excellent quality original data to performance a clinical useful post-processing image. Post-processing is achieved by using morphological mathematics to remove spurious image elements.

Morphology is a broad set of mathematical operations that processes an image based on the shapes. Morphological operations apply a structuring element on an input image after converting it into binary form to get an output image of the same size. The basic morphological operations are **dilation** which adds pixels to the boundaries of objects in an image; the value of the output pixel is the maximum of all the pixels in the input pixel's neighborhood (If any of the pixels is set to the value 1, the output pixel is set to 1), and **erosion** which removes pixels on object boundaries; the value of the output pixel is the minimum value of all the pixels in the input pixel's neighborhood (If any of the pixels is set to 0, the output pixel is set to 0). The aim of these operations is to show only the tumor's part in the image and the purpose of this step is to improve the segmented image.

## II.8. 3D Reconstruction using Marching Cube Algorithm

Three dimensional (3D) reconstruction of the tumor from medical images is an important operation in the medical field as it helps the radiologist in the diagnosis, surgical planning and biological research. Thus in this section, we propose an effective and efficient approach to 3D reconstruction of brain tumor and estimation of its volume from a set of two dimensional (2D) cross sectional magnetic resonance (MR) images of the brain.

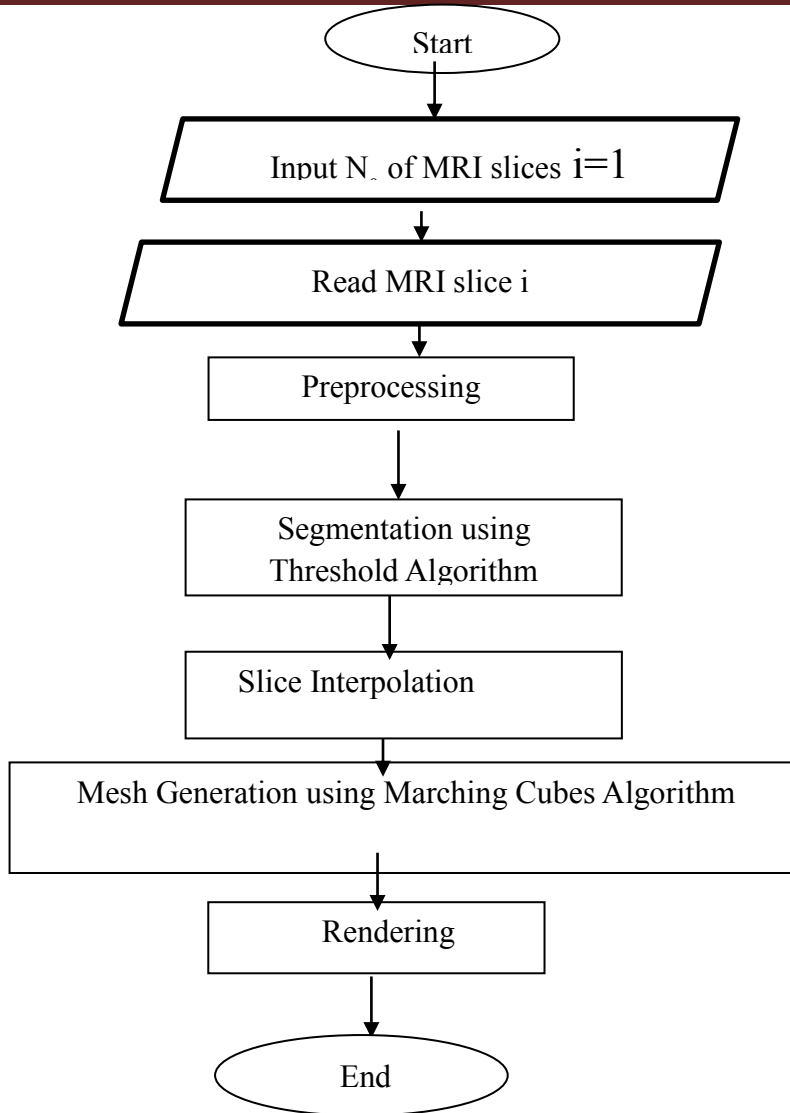
Representation of a 3D data in the form of 2D projected slices does result in loss of information and may lead to erroneous interpretation of results [2]. Also, 2D images cannot accurately convey the complexities of human anatomy and hence interpretation of complex anatomy in 2D images requires special training. Although radiologists are trained to interpret these images, they often find difficulty in communicating their interpretations to a physician,

who may have difficulty in imagining the 3D anatomy. Hence, there is a need for 3D reconstruction of the tumor from a set of 2D parallel cross sectional images. 3D visualization enables better understanding of the topology and shape of the tumor, facilitate the measurements of its geometrical characteristics. The extracted information is helpful in staging of tumor, surgical planning, and biological research [3]. Therefore, reconstructing a trustworthy surface from the sequential parallel 2D cross sections using python simulator becomes a crucial issue in biomedical 3D visualization.

- The brain MR images have unique characteristics, i.e., very complicated changes of the gray-scales and highly irregular boundaries. Traditional 3-D reconstruction algorithms are challenged in solving this problem. Many reconstruction algorithms, such as marching cubes and dividing cubes, need to establish the topological relationship between the slices of images. The results of these traditional approaches vary depending on the number of input sections, their positions, the shape of the original body and the applied interpolation technique. These make the task tedious and time-consuming.

## **II.9. Proposed Methodology**

The part of the image containing the tumor normally has more intensity than the other portion and the area, shape and radius of the tumor in the image can be very well known. These basic conditions are utilized to detect the tumor. The main task of 3D reconstruction of the tumor from a set of 2D parallel cross sectional images is divided into several subtasks as shown in Figure (II.7)



**Figure II.4:** Flowchart of the Proposed 3D Tumor Reconstruction Approach

### II.9.1. Pre processing of different slices

Image pre-processing can significantly increase the reliability of an optical inspection. To get more surety and ease in detecting the tumor, it is useful because the quality of the input data cannot be acceptable, therefore it usually needs to be improved. In preprocessing some basic image enhancement (After noise reduction, the edge-enhanced image is added to the original image to increase the visual quality of the image) and noise (can mask and blur the important features in the MR image and thus make the further steps in medical image analysis difficult) reduction techniques are used. The aim to of this step is to improve the quality of the image.

As the analysis has to be performed on brain region, the skull region is eliminated from each MR images of the brain by converting original MR image to a binary image and retaining only the pixels in the largest connected component which corresponds to the brain region.

### **II.9.2. Extraction of tumor in different slices**

Image segmentation can be performed sequences of 2D images, or 3D volumetric imagery. Most of the image segmentation research has focused on 2D images. If the data is defined in 3D space (e.g, obtained from a series of MRI images), then typically each image (slice) is segmented individually in a (slice-by-slice) manner. This type of segmenting 3D image volumes often requires a post-processing step to connect segmented 2D slices into a 3D volume or a continuous surface. Moreover, the resulting segmentation can contain inconsistencies and nonsmooth surface due to omitting important anatomical information in 3D space. Therefore, the development of 3D segmentation algorithms is desired for more accurate segmentation of volumetric imagery. In practice, 2D image segmentation methods can be extended to 3D space, but often with the cost of an increased complexity of the method and slower computational time.

The goal of image segmentation is to divide an image into a set of semantically meaningful, homogeneous, and nonoverlapping regions of similar attributes such as intensity, depth, color, or texture.

### **II.9.3. Slice Interpolation**

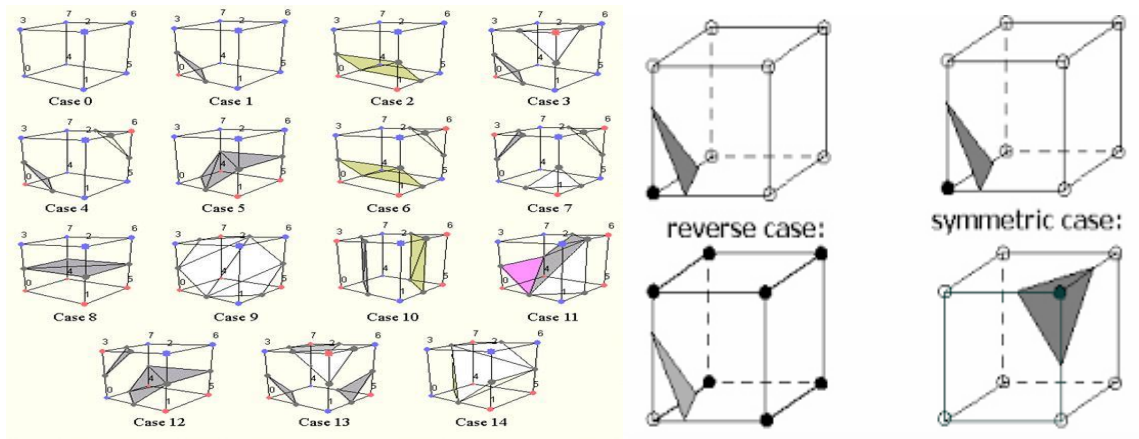
After the segmentation, slices of the segmented tumor are stacked up to form the volume data in the 3D space. Generally, the set of slices acquired from the MRI device is such that the distance between the slices is larger than the distance between the pixels within the slice. The surface reconstructed with such a set of slices is inaccurate and not smooth. Thus in this work, the missing slices are estimated using interpolation technique.

### **II.9.4. Mesh generation using Marching cubes**

A three-dimensional surface is a representation of volumetric image data in a shape form. One algorithm, which is acceptable for reconstructing those surfaces, is the Marching cubes. It uses patterned cubes or isosurface to approximate contours. The marching cubes algorithm needs some processes or algorithms to reduce time and memory for reconstructing a surface from large volumetric data. There are two primary steps in our approach to the surface construction problem. First, we locate the surface corresponding to a user-specified value and

create triangles. Then, to ensure a quality image of the surface, we calculate the normals to the surface at each vertex of each triangle.

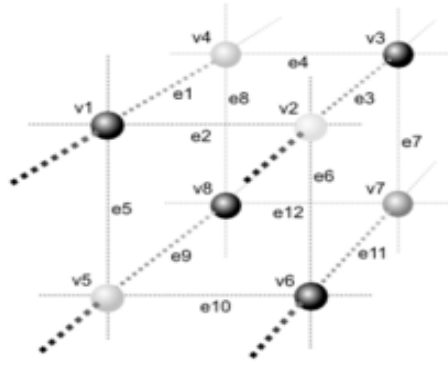
The algorithm determines how the surface intersects this cube then moves to the next cube. There are 8 vertices which are inside or outside the surface that means we are working with  $2^8$  or 256 different probabilities for what a cube might look like. Triangulating the 256 cases might be a pain but luckily, given identical triangulations for cubes whose vertex classification is opposite of each other, rotations and mirroring, there are in fact only 14 unique triangulations. Each triangulation contains 0 to 4 triangles and can be stored as a list of triangles where each triangle is a list of 3 numbers which are indexes to the edges on which each triangle vertices lie. Figure (II.8) shows the triangulation for the 14 patterns.



**Figure II.5:** Triangulated Cubes.

The cube vertices receive a zero and they're outside the surface if they have a value below the surface. The surface intersects those cube edges where one is outside the surface (1) and the other is inside (0).

We create an index for each case, based on the state of the vertex, which serves as a pointer into an edge table that gives all edge intersections for a given cube configuration. Using the vertex numbering in Figure (II.9), the eight bit index contains one bit for each vertex.



**Figure II.6:** Cube Numbering.

Using the index to tell which edge the surface intersects, we can interpolate the surface intersection along the edge. We use linear interpolation, but have experimented with higher degree interpolations. Since the algorithm produces at least one and as many as four triangles per cube, the higher degree surfaces show little improvement over linear interpolation. The final step in marching cubes, calculates a unit normal for each triangle vertex. The rendering algorithms use this normal to produce Gouraud-shaded images.

In summary, marching cubes creates a surface from a three-dimensional set of data as follows:

- Read four slices into memory.
- Scan two slices and create a cube from four neighbors on one slice and four neighbors on the next slice.
- Calculate an index for the cube by comparing the eight density values at the cube vertices with the surface constant.
- Using the index, look up the list of edges from a precalculated table.
- Using the densities at each edge vertex, find the surface edge intersection via linear interpolation.
- Calculate a unit normal at each cube vertex using central differences. Interpolate the normal to each triangle vertex.
- Output the triangle vertices and vertex normals.

### II.9.5. Rendering

At this stage which is the final step, realistic effects are added to the surface of the 3D model by applying Phong lighting and shading model [4]. First the normals of the triangle vertices in the mesh are computed by taking the average of the adjacent triangle normals. Then the shading model linearly interpolates the vertex normal and then applies the lighting

model at each point on the surface to determine the intensity at that point and thus shades the entire surface.

### **II.10. Summary**

Detection brain tumor in MRI in a fast, accurate, and reproducible way is a challenging problem. Automatic image segmentation has become very important aspect for realizing content based image description. Many algorithms are used in order to segment the image and depict the abnormal tissues on rapid and effective way. In this chapter, first, a brain tumor segmentation method has been developed and validated on 2D MRI data. The visualization of the segmentation results demonstrate the effectiveness of this approach, and then we described an effective approach for detection and 3D reconstruction of brain tumor using the marching cube algorithm for assisting the physician in surgical planning. It is very well suited to 3D surface reconstruction. Given a surface for which you can test arbitrary points for whether they fall inside or outside the object, it's only weakness is occasional extraneous triangles. It is fast (linear increases in time as area increases), accurate and works with arbitrarily shaped objects. With slice data it's only additional weakness is a stair stepping effect when the surface approaches parallel with the slices. Both of these weaknesses can be overcome with post-processing.

# Chapter III

## Texture analysis

---

The analysis of texture parameters is a useful way of increasing the information obtainable from medical images. It is an ongoing field of research, with applications ranging from the segmentation of specific anatomical structures and the detection of lesions, to differentiation between pathological and healthy tissue in different organs. Texture analysis uses radiological images obtained in routine diagnostic practice, but involves an ensemble of mathematical computations performed with the data contained within the images.

---

### III.1. Introduction

Texture analysis is the extraction of textural features from images. The meaning of texture varies, depending on the area of science in which it is used. In image processing it is an essential issue that comprises a set of mathematical techniques used to quantify the different gray levels within an image in terms of intensity and distribution. In this chapter we are going to clarify the principles of texture analysis and give examples of its applications and some of the disciplines in which it is use.

### III.2 Texture analysis

Texture analysis refers to the branch of imaging science that is concerned with the description of characteristic image properties by textural features.

In image analysis, it is defined as a function of the spatial variation in intensities of pixels patterns that reproduce the data of gray level statistics, anatomical intensity variations, texture, spatial relationships, shape, structure and so on. Moreover it is considered as a useful computational method for discriminating between pathologically different regions on medical images because it has been proven to perform better than human eyesight at discriminating certain classes of texture. Two contrasting methods are presented for evaluating the performance of the texture analysis methodologies: First and Second-Order Statistical Texture Analysis

#### III.2.1 First-Order Statistical Texture Analysis

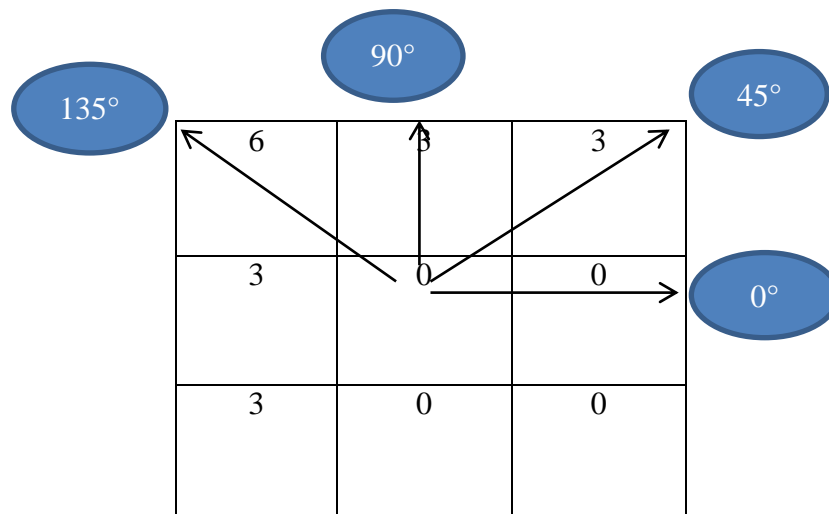
First-order texture analysis measures, to calculate texture, image histogram, or pixel occurrence probability is used. The main advantage of this approach is its simplicity through the use of standard descriptors (e.g. mean and variance) to characterize the data. However, the power of the approach for discriminating between unique textures is limited in certain applications because the method does not consider the spatial relationship, and correlation, between pixels. For any surface, or image, grey-levels are in the range  $0 \leq i \leq N_g-1$ , where  $N_g$  is the total number of distinct grey-levels. If  $N(i)$  is the number of pixels with intensity  $i$  and  $M$  is the total number of pixels in an image, it follows that the histogram, or pixel occurrence probability, is given by,

$$P(i) = \frac{N(i)}{M} \quad \text{(III.1)}$$

In general seven features commonly used to describe the properties of the image histogram, and therefore image texture, are computed. These are: mean; variance; coarseness; skewness; kurtosis; energy; and entropy.[]

### III.2.2 Second-Order Statistical Texture Analysis

The human visual system cannot discriminate between texture pairs with matching second order statistics (Julesz, 1975). The first machine-vision framework for calculating second-order or pixel co-occurrence texture information was developed for analyzing aerial photography images (Haralick et al., 1973). In this technique pixel co-occurrence matrices, which are commonly referred to as grey level co-occurrence matrices (GLCM), are computed. The entries in a GLCM are the probability of finding a pixel with grey-level  $i$  at a distance  $d$  and angle  $\theta$  from a pixel with a grey-level  $j$ . This may be written more formally as  $P(i, j : d, \theta)$ . An essential component of this framework is that each pixel has eight nearest-neighbours connected to it, except at the periphery. As a result four GLCMs are required to describe the texture content in the horizontal ( $P_H=0^\circ$ ), vertical ( $P_V=90^\circ$ ) right- ( $P_{RD}=45^\circ$ ) and left-diagonal ( $P_{LD}=135^\circ$ ) directions. This is illustrated in Fig(III.7)[]



**Figure III.1:** Example of GLCM showing the different direction of  $\theta$

### III.2.2.1 The grey Level Co-occurrence Matrix

A statistical method of examining texture that considers the spatial relationship of pixels is the gray-level co-occurrence matrix (GLCM), also known as the gray-level spatial dependence matrix. This last characterizes the texture of an image by calculating how often a pixel with the intensity (gray-level) value  $i$  occurs in a specific spatial relationship to a pixel with the value  $j$  in a specified spatial relationship, creating a GLCM, and then extracting statistical measures from this matrix. By default, the spatial relationship is defined as the pixel of interest and the pixel to its immediate right (horizontally adjacent), but you can specify other spatial relationships between the two pixels. Each element  $(i,j)$  in the resultant glcm is simply the sum of the number of times that the pixel with value  $i$  occurred in the specified spatial relationship to a pixel with value  $j$  in the input image. To create a GLCM, use the `graycomatrix` function. The `graycomatrix` function creates a gray-level co-occurrence matrix (GLCM) by calculating. The number of gray levels in the image determines the size of the GLCM. By default, `graycomatrix` uses scaling to reduce the number of intensity values in an image to eight, but we can use the `NumLevels` and the `GrayLimits` parameters to control this scaling of gray levels.

### III.3. GLCM parameters

Haralick et al. proposed a large number of features called Haralick's texture features [2] derived from the co-occurrence which reflects different property in the image.

#### III.3.1 Contrast

Returns a measure of the intensity (the local variations of gray levels) between a pixel and its neighbor over the whole image. This parameter can also characterize the dispersion of the matrix values from its main diagonal. Images with large neighboring gray level differences are associated with high contrast. It is defined as follows:

$$\text{Cont} = \sum_{i,j} |i - j|^2 p(i, j) \quad (\text{III.2})$$

Where  $P(i, j)$  corresponds to the probability of moving from a pixel with gray level  $i$  to a pixel with gray level  $j$ . Contrast is 0 for a constant image.

#### III.3.2 Correlation

Returns a measure of how correlated a pixel is to its neighbor over the whole image.

$$\mathit{corr} = \sum_{i,j} \frac{(i-\mu_i)(j-\mu_j)p^2(i,j)}{\sigma_i\sigma_j} \quad (\text{III.3})$$

Correlation is 1 or -1 for perfectly positively or negatively correlated image. Correlation is NaN for a constant image.

### III.3.3 Energy

Returns the sum of squared elements in the GLCM. it reflects pixel-pair repetitions. Homogeneous images have very few dominant gray tone transitions, which result into higher energy. Energy is 1 for a constant image. Energy is defined as follows :

$$\mathit{energy} = \sum_{i,j} p(i,j)^2 \quad (\text{III.4})$$

### III.3.4 Homogeneity

Returns a value that measures the closeness of the distribution of elements in the GLCM to the GLCM diagonal. It assigns larger values to smaller gray level differences within pixel pairs. This parameter has opposite behavior of the contrast. More the texture has homogeneous regions, more the parameter is high. Homogeneity is 1 for diagonal GLCM.

$$\mathit{hom} = \sum_{i,j} \frac{p(i,j)}{1+|i-j|} \quad (\text{III.5})$$

### III.3.5 Entropy

It is a measure of non-uniformity in the image or region of interest. If the image is heterogeneous, many elements on the co-occurrence matrix have small values, which imply that entropy is very large. Entropy is inversely correlated to energy, it is given by the following expression:

$$\mathit{ent} = -\sum_{i,j} p(i,j)(\log p(i,j)) \quad (\text{III.6})$$

### III.3.5 Mean

The mean is determined by the homogenous brightness or darkness of the image. The more homogeneously bright the image is, the higher is its mean, and vice versa. The mean is written as:

$$\mathit{mean} = \sum_{i,j} p(i,j) \quad (\text{III.7})$$

### III.3.6 Variance

It is a measurement of heterogeneity and was correlated strongly with standard deviation. It characterizes the distribution of gray levels around the mean value calculated above. Therefore, variance increased when the gray levels values differed from their means.

The expression of the variance is:

$$Var = \sum_{i,j} (i - mean)^2 p(i,j) \quad (\text{III.8})$$

### III.4 Summary

In this chapter, we started by introducing the principle of the texture analysis. Then, we dealt with different approaches used in this analysis moreover we discussed about the gray level co-occurrence matrix and the different parameters which reflects different property from the image.

# Chapter IV

## Results and Discussion

---

In the first section, the performance of threshold segmentation and clustering algorithms have been applied to different MRI images containing the tumor, in order to obtain the desired portion or region and different classes, after applying algorithm explained before, all the thresholding values of different methods , tumor's surfaces and areas can be calculated then the tumor image after post processing using morphological operations listed previously have been obtained and used to reconstruct them on 3D modeling. In the last section texture analysis is presented and applied for different regions of an MRI in order to improve discriminating between several tissues.

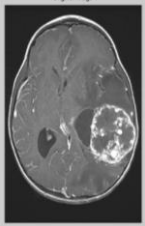
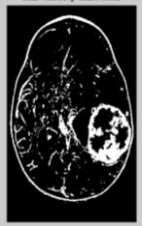

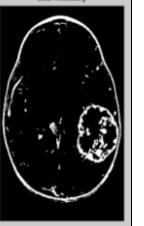
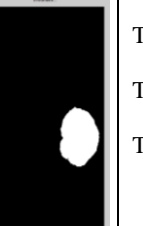
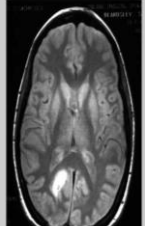


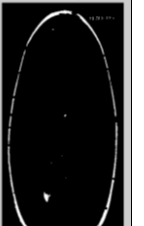
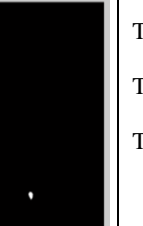
---

## IV.1. Comparative study of segmentation method on brain tumor's extraction

### IV.1.1. Thresholding processing

Thresholding technique segment scalar images by generating a binary partitioning of the image intensities. It tries to find an intensity value, called the threshold, which separates the desired classes. The segmentation is then obtained by grouping all pixels with intensity greater than the threshold into one class, and all other pixels into another class. In this step, the region between the skull and the brain tissue will be determined and this region to be segmented has considerable different grey values with other tissues. This proposed approach uses Otsu thresholding technique which is used to automatically carry out the lessening of grey-level image to a binary image. After applying the threshold algorithm to a set of MRI images, the tumor has been extracted, the statistical tumor surface and area have been calculated.

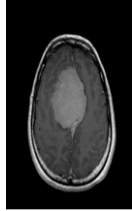




The table below shows the results of the threshold algorithm applied for tumor extraction and its statistics.

Original MRI Image	Threshold Methods			Tumor Alone	Parameter results		
	Iterative	Otsu	Local		Threshold Values	Tumor Surface	Areas
					$T_I=0.5144$ $T_O=0.3216$ $T_L=0.2706$	$T_S = 7679$	$A=7697.4$
					$T_I = 0.3120$ $T_O = 0.2471$ $T_L = 0.3961$	$T_S = 152$	$A=154.75$

**Table IV.1:** Results of Threshold Algorithm for tumor extraction.

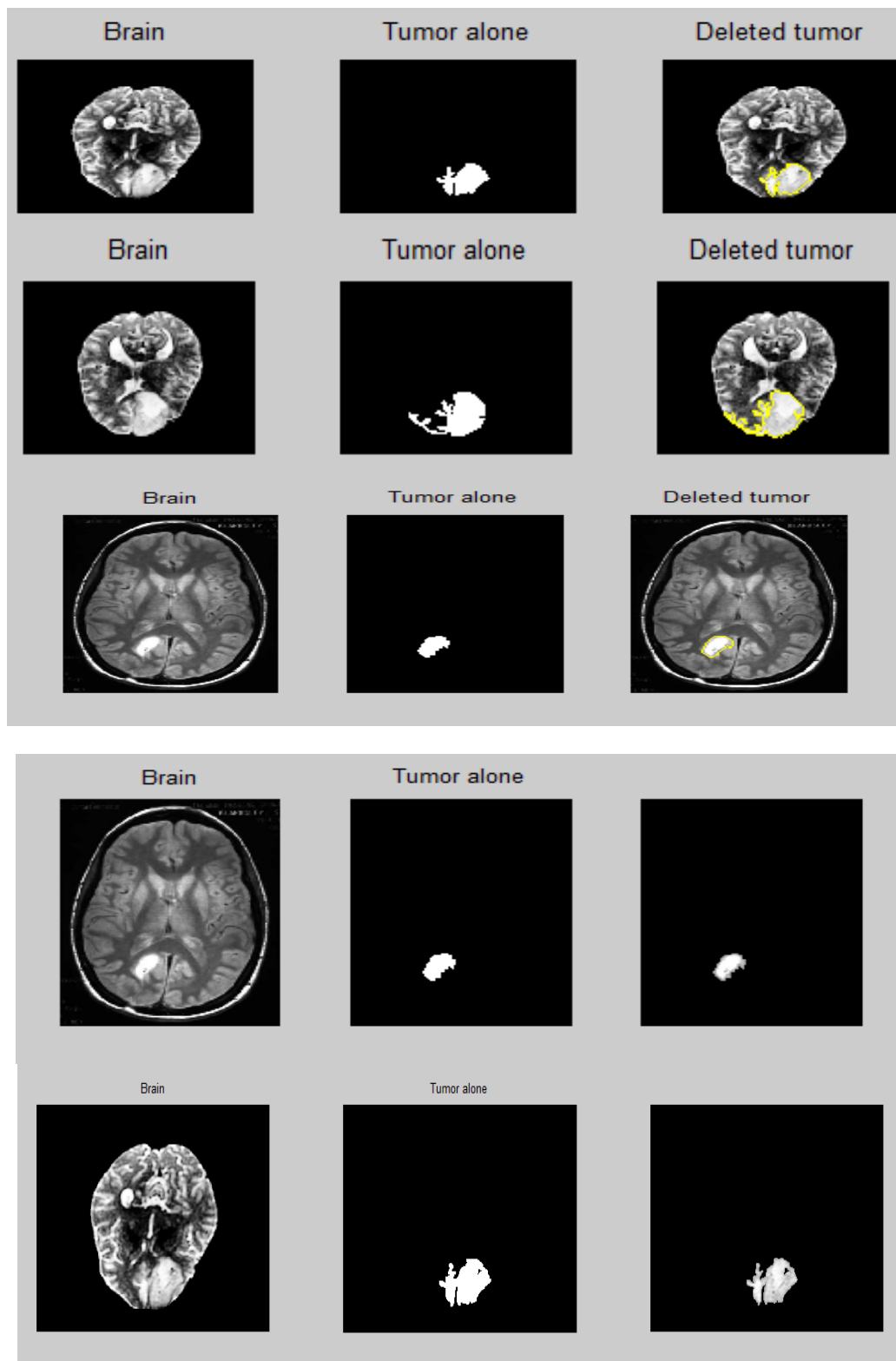
The range of values permitted for the thresholds is between 0 and 1, any given value higher or lower will cause the system to return error.

Sometimes the user can not completely remove the skull in preprocessing this may cause the system to treat the skull also as a lesion and compute the area wrong as shown in the following table:

Original MRI Image	Threshold Methods			Tumor Alone	Parameter results		
	Iterative	Otsu	Local		Threshold Values	Tumor Surface	Areas
					$T_I=0.3102$ $T_O= 0.1922$ $T_L=0.3137$	$T_S = 6839$	$A=6921.8$

**Table IV.2:** Results of Threshold Algorithm for tumor extraction with mistakes

According to the result, we remark that the program detects the skull as a tumor, therefore the surface and the area calculations are wrong because the skull is considered as a tumor due to its characteristics. After improving our code, by using post-processing step, we got the following results:

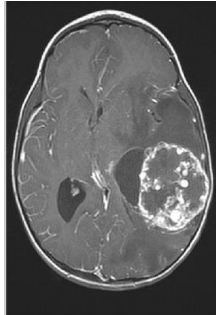
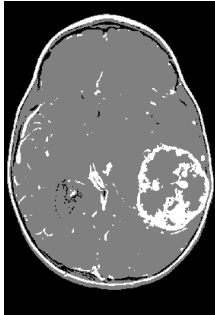
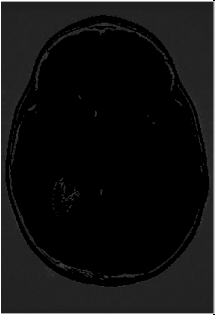
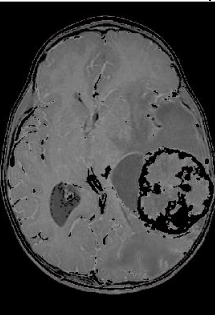
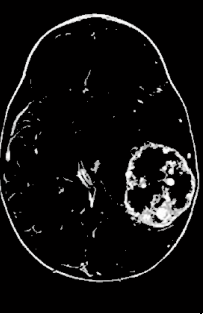





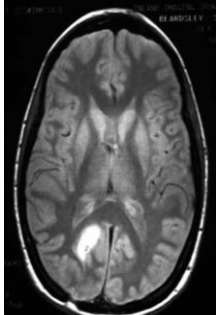


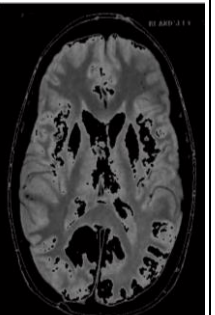

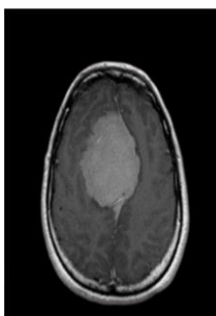
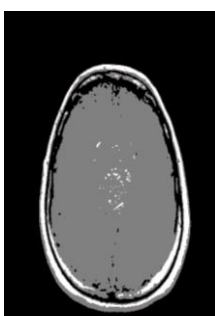
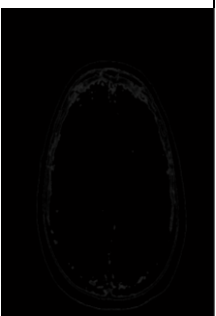
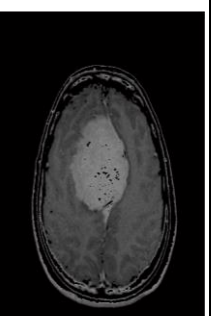



**Figure IV.1:** Results of improved Threshold Algorithm for tumor extraction

**IV.1.2. K-Means processing**

For the classification of the image, the K-Means and FCM clustering can be adopted to identify the potential abnormal regions (Tumor in our case).After clustering, a separation of clusters is done. After applying the clustering algorithm to a set of MRI images, the tumor has been extracted.

The table below shows the results of the K-Means algorithm that is applied for tumor extraction.

Original MRI Image	K-Means Method			
	Clustered MRI Image	Objects in Cluster 1	Objects in Cluster 2	Objects in Cluster 3
				
				
				
				

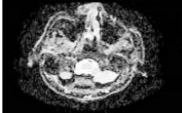
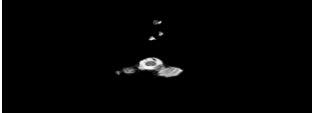
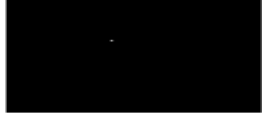

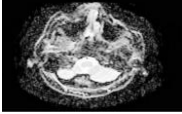


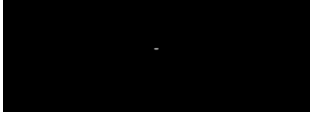
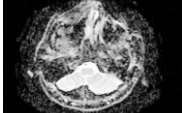

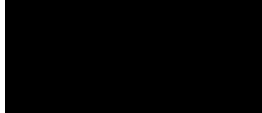
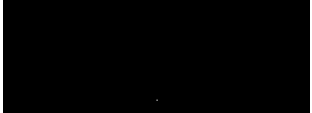
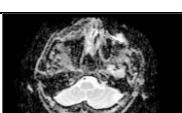



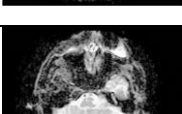



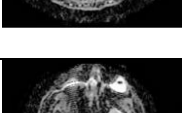



**Table IV.3:** Results of K-Means Algorithm for tumor extraction

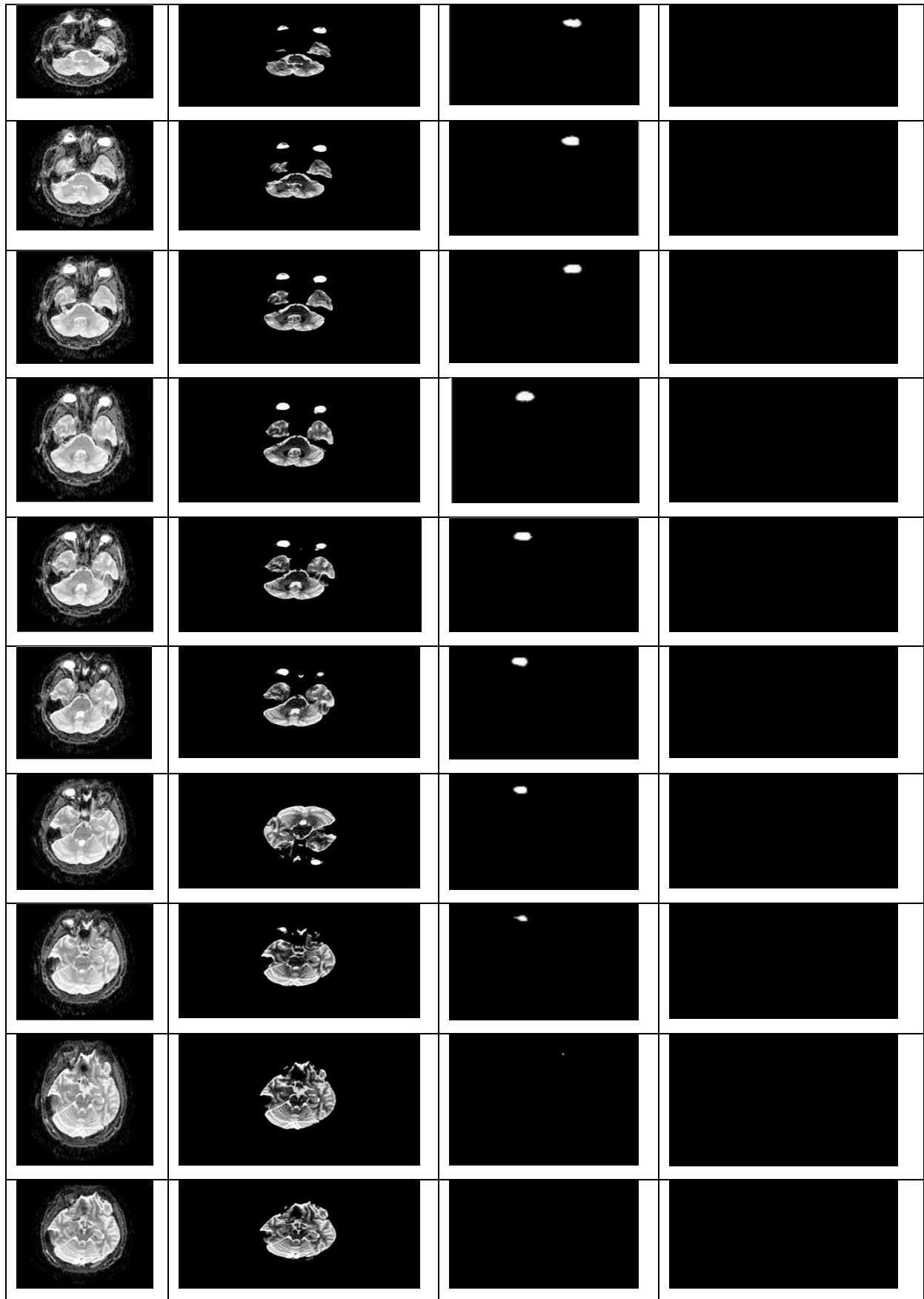
From the results obtained, we deduced that K-Means gives better results for abnormal tissue recognition. The thresholding and Otsu give better results for the bone structure (skull)

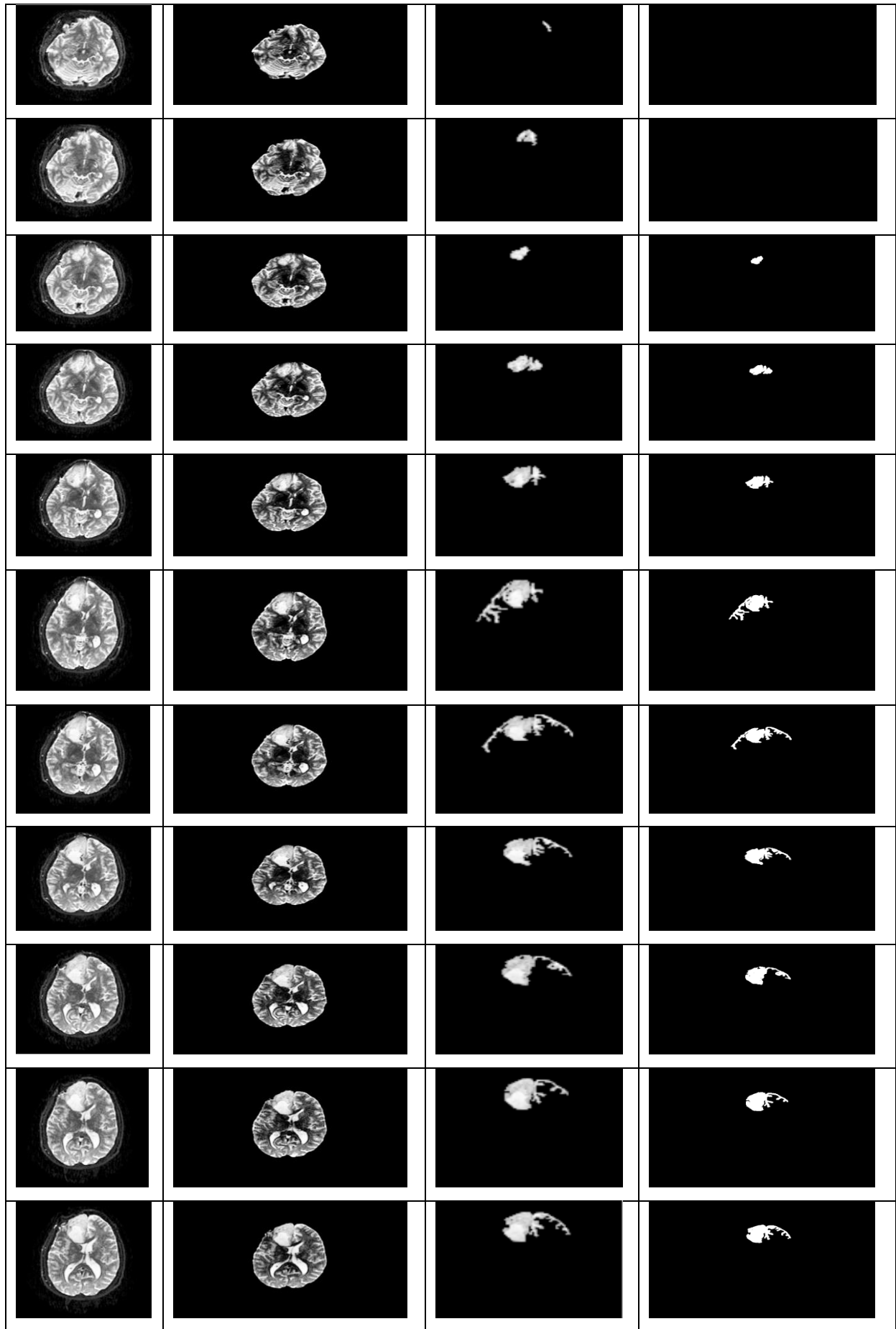
extraction. Therefore, to get the accurate results in the segmentation, we have to use the post-processing step.

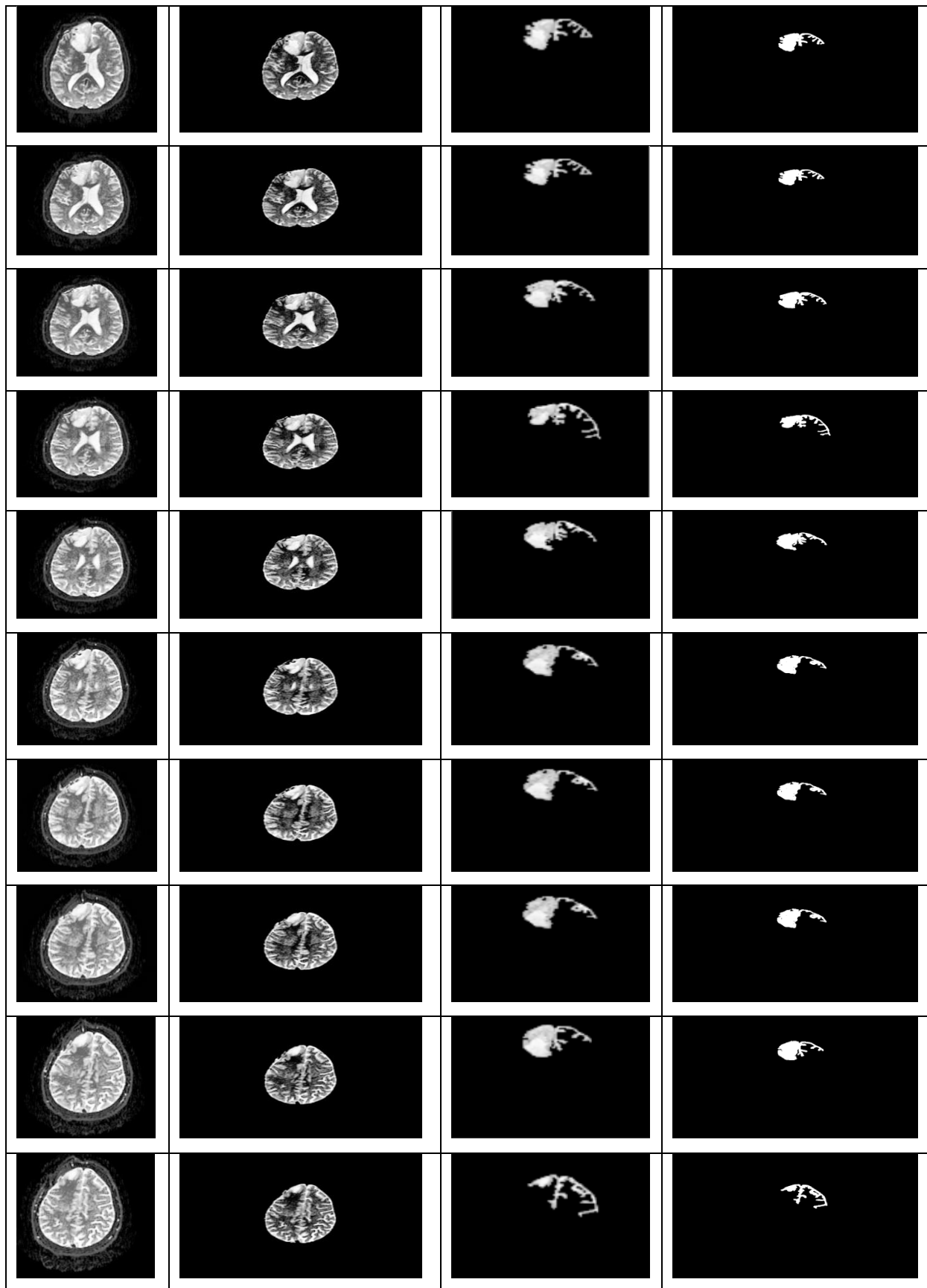
## IV.2. Marching Cube algorithm Results

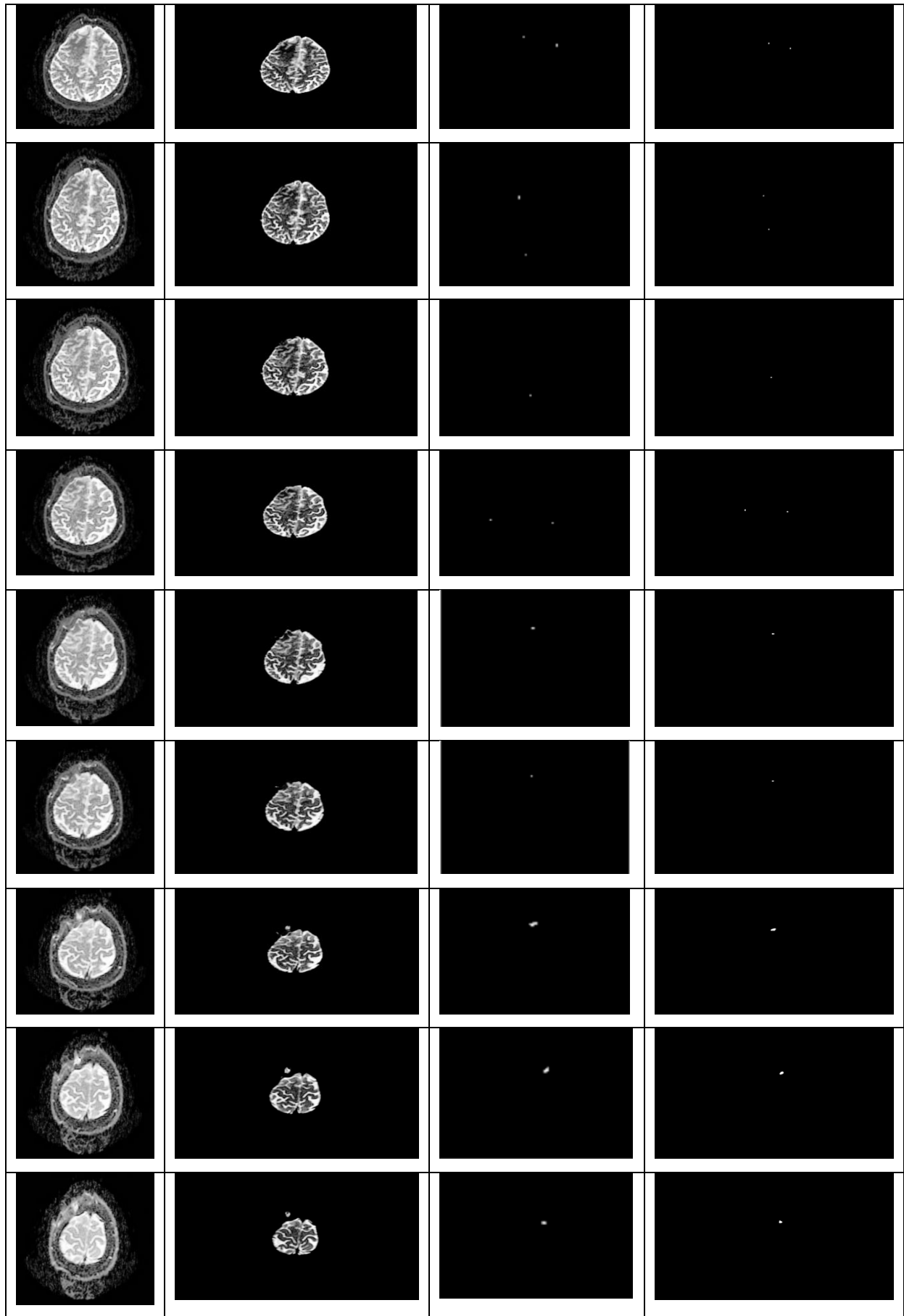
Sets of images exported from the net in DICOM (Digital Imaging and Communications in Medicine) standard were placed at our disposal which having greater resolution. The set consists of 51 slices with 800x600 pixels for a single image size, which are grayscale and compressed with JPEG compression, in coronal plain. We implement the Marching Cube Algorithm for detection and 3D-reconstruction of brain tumor, the following steps describe the overall architecture of the processing of the system. First it starts with the loading of the MRI brain image, which is considered as an input image. The pre-processing of this input image takes place i.e., the enhancement of the image. After that the segmentation stage, first the tumor pixels are identified then extracted. Before the 3D reconstruction is displayed, the post-processing step is involved in order to get better results for segmentation. The table below explains the steps of the proposed system:

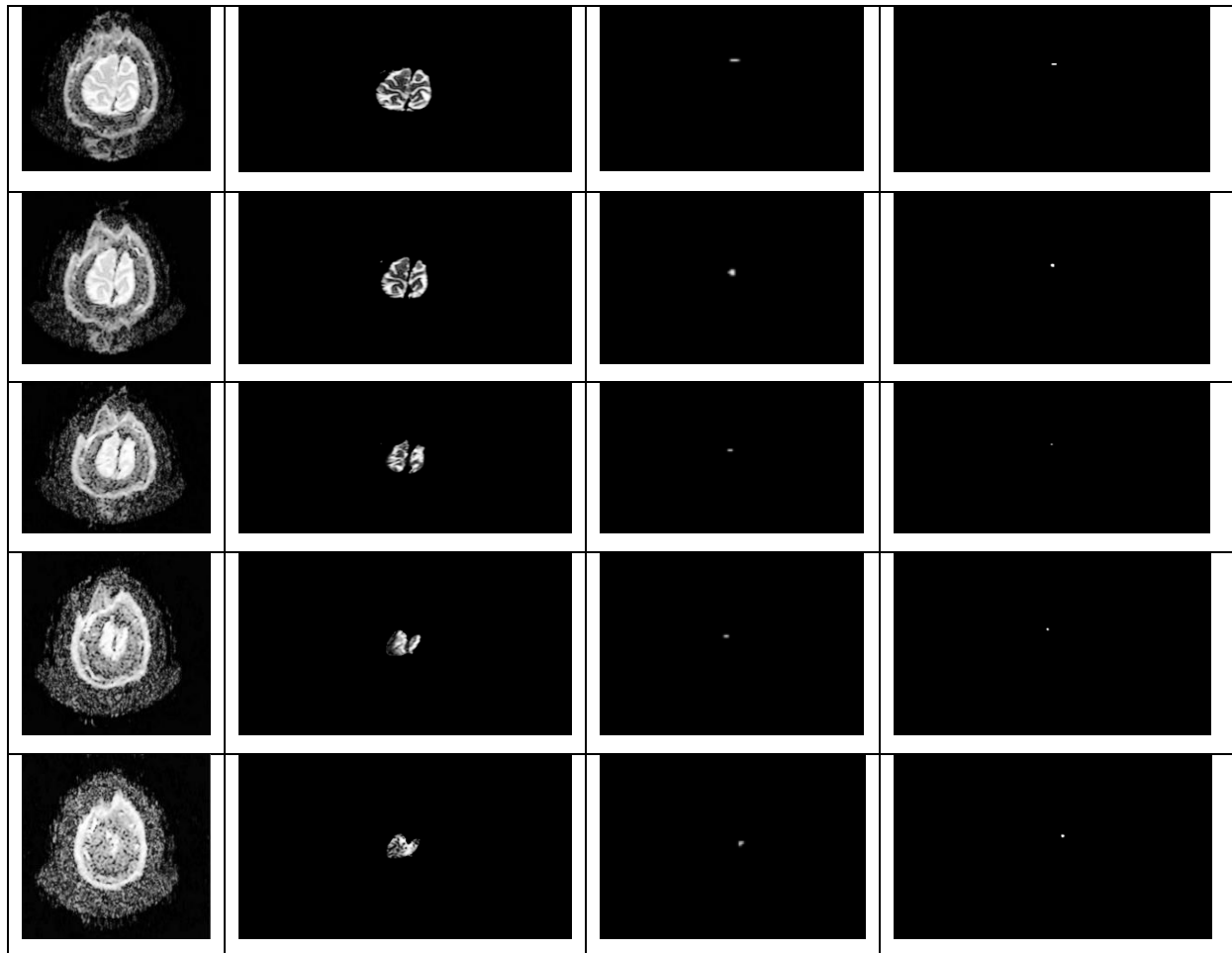
Original Slice's Images	Pre-processed slices	Segmented slices	Post-processed slices
			
			
			
			
			
			









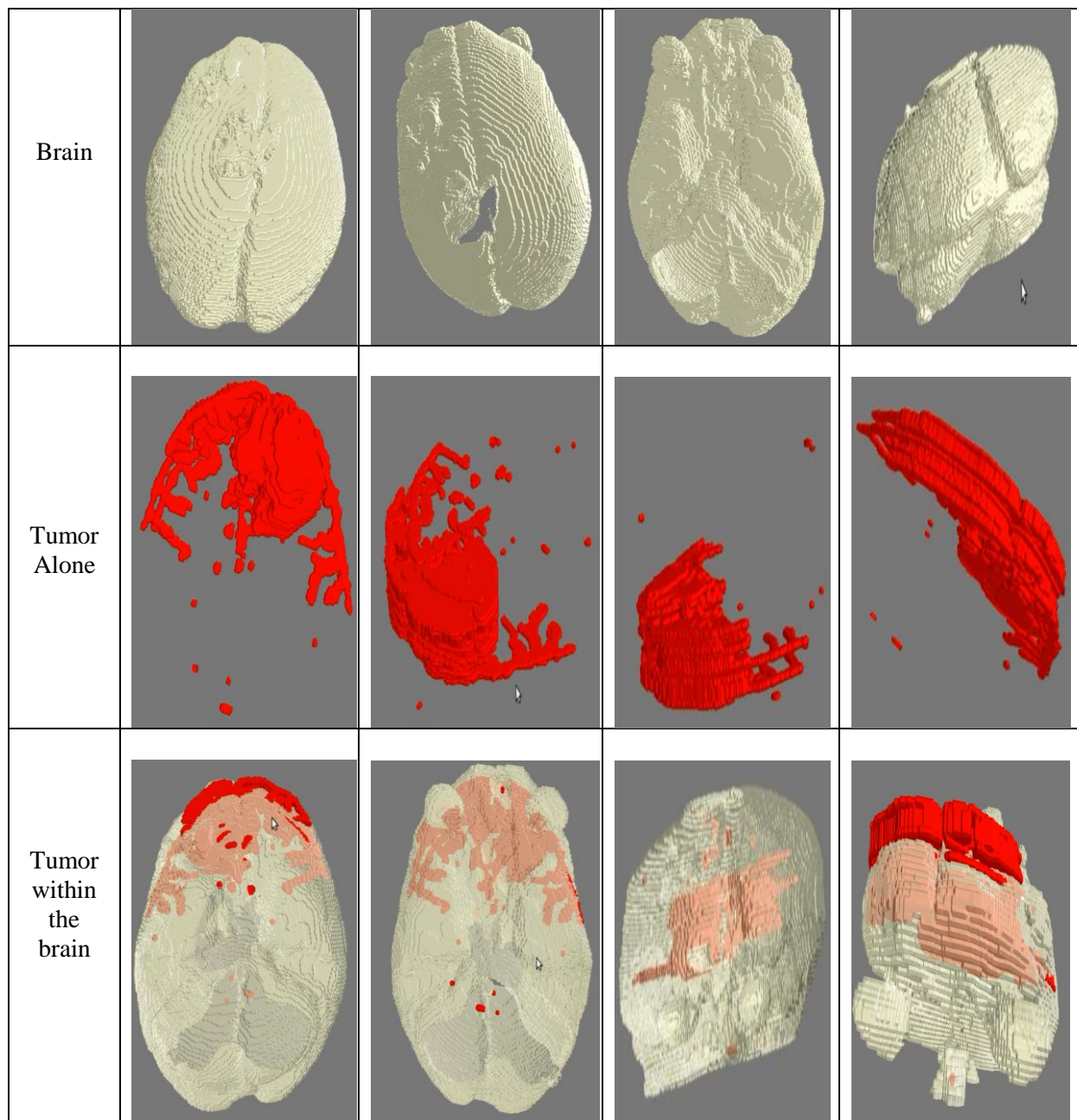


**Table IV.4:** Results of the steps used for tumor extraction.

We have applied the Pre-processing step before the segmentation process for the improved segmented output which will not be affected by the noise. Intracranial area is extracted from the images (sometimes the bone structure is absent in MRI images) by applying threshold, otsu and logical operators to the enhanced images, and to eliminate the background and skull from the intracranial area, we set their pixel values to zero (black pixel). After that we have segmented the result of the Pre-processing images in order to extract the tumor's region.

In some slices, we have extracted the eyes as an abnormal tissue due to its intensity means that they have the same grey level; as a result we have introduced the Post-processing step where we have used morphological operations in order to eliminate the eyes which are located in the slices. Finally, the 3D reconstruction of the abnormal's tissue in brain MRI images is obtained by implementing the Marching Cube Algorithm.

The table below shows the 3D tumor reconstruction, where we put the tumor and the brain in the same frame work in order to get the two parts together.



**Table IV.5:** 3D Reconstruction using marching cube.

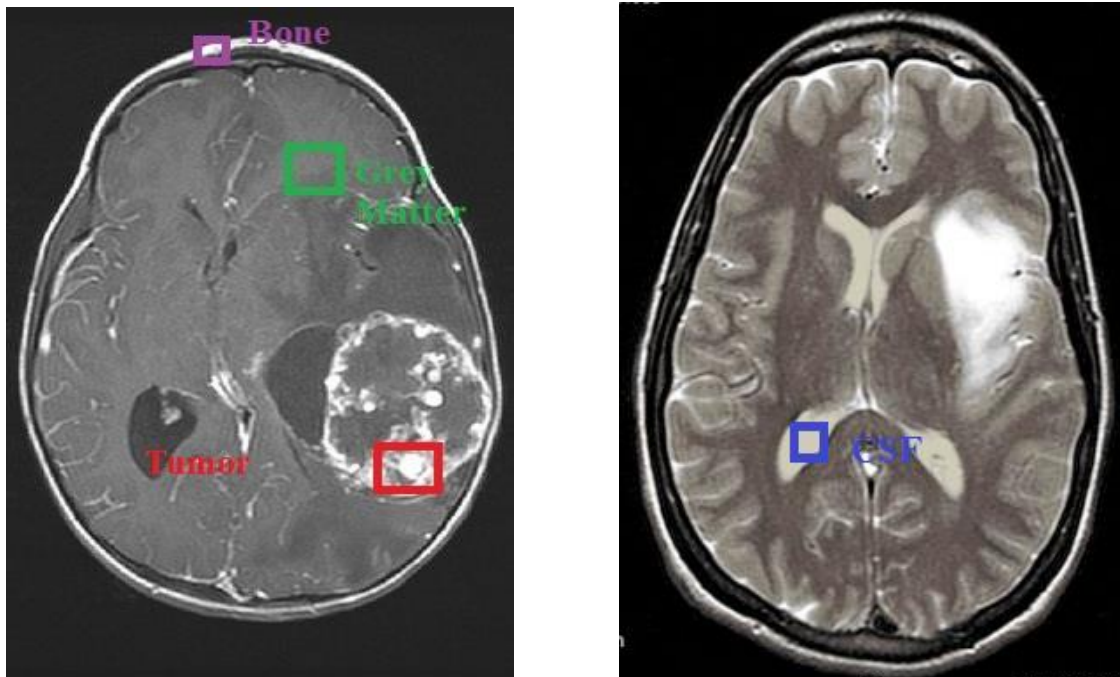
The reconstructed tumor is the Glial one which is infiltrative tumor with no clear indication, it is surrounded by the edema and Gliosis.

The approach used depends on the type of the tumor that is used and its location (intra/extra/deeper and superficial level); it works well i.e., it extracts the tumor alone when it is well limited and it extracts both the tumor and Gliosis when the tumor is spreads; in this

case the extraction is difficult as in medicine because sometimes the Gliosis becomes the future tumor.

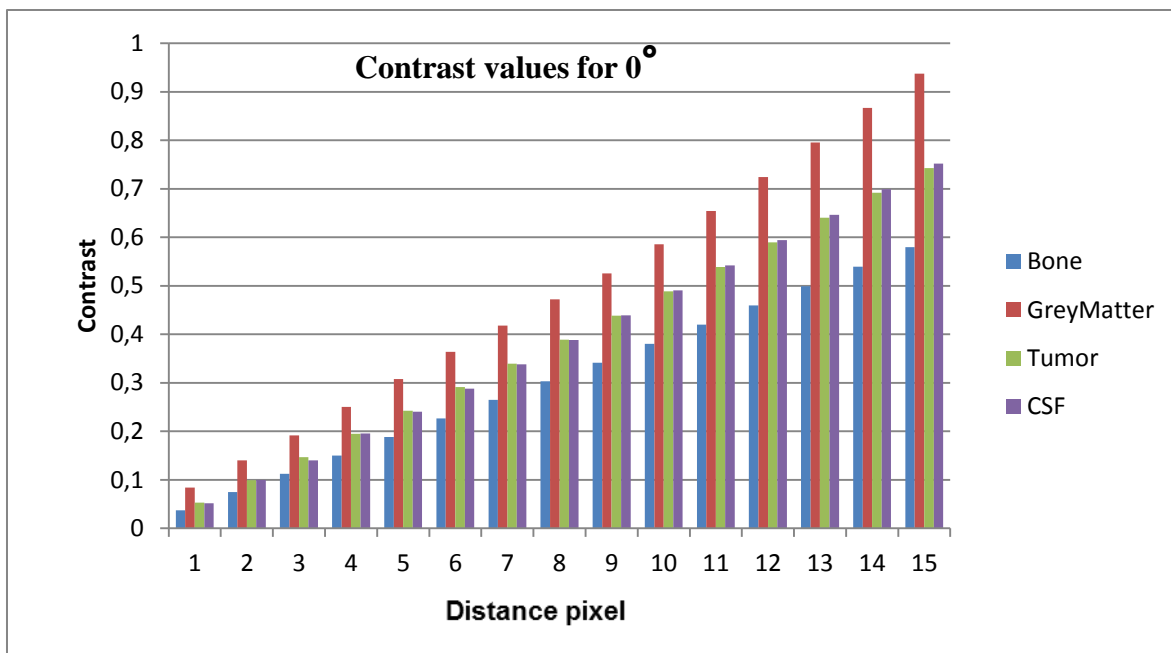
### IV.3. Texture analysis procedure

In this section texture analysis have been applied for four different samples of an MRI image in order to characterize each region based on the study of several parameters, therefore these samples are shown as follow:

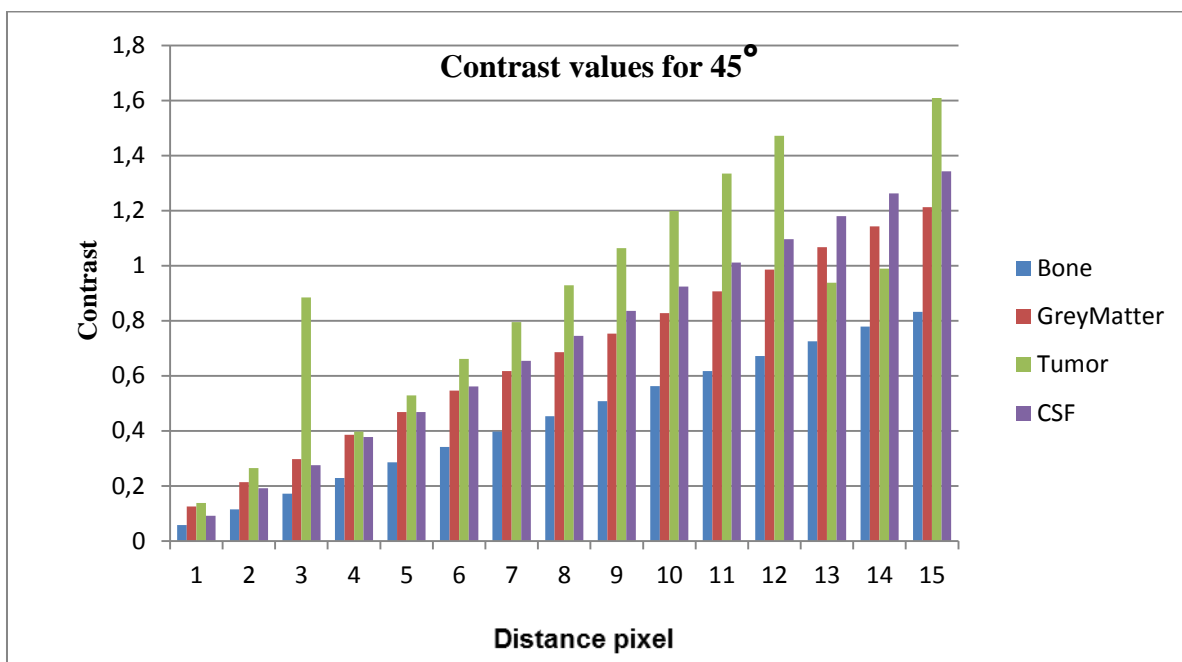


**Figure IV.2:** The four samples used in the texture analysis

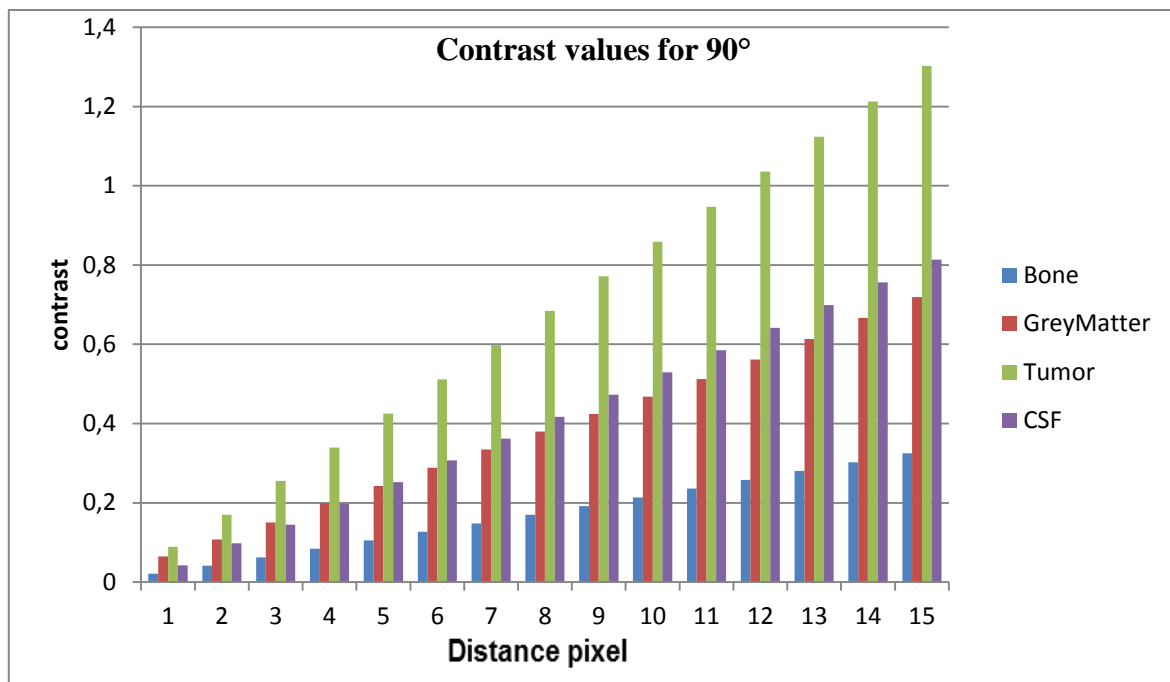
After selecting manually four rectangular regions to calculate textural features derived from the GLCM, five Haralick's descriptors for GLCM computation were calculated using different offsets and different angles. The results are shown in the following graphs:



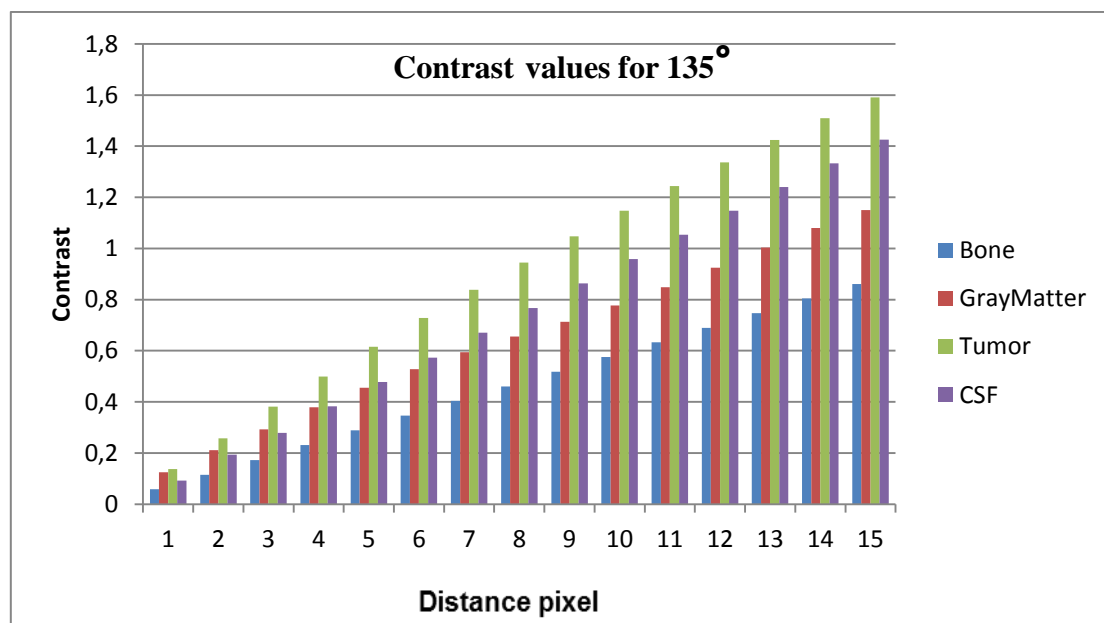
**Figure IV.3:** Contrast values for different samples (Bone, GreyMatter, Tumor, CSF) with  $\theta=0^\circ$



**Figure IV.4:** Contrast values for different samples (Bone, GreyMatter, Tumor, CSF) with  $\theta=45^\circ$

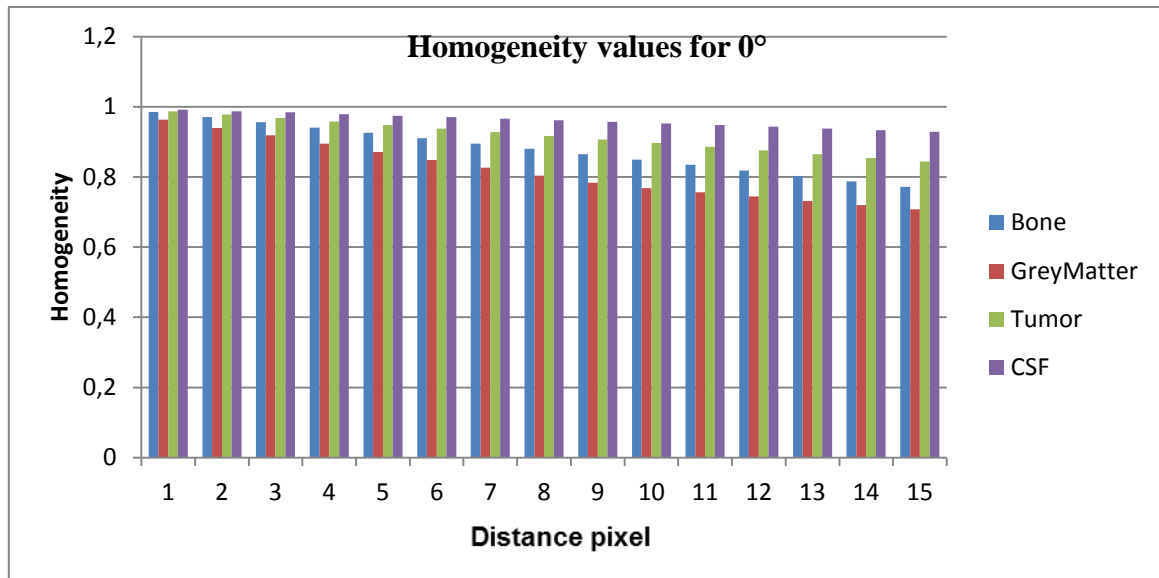


**Figure IV.5:** Contrast values for different samples (Bone, GreyMatter, Tumor, CSF) with  $\theta=90^\circ$

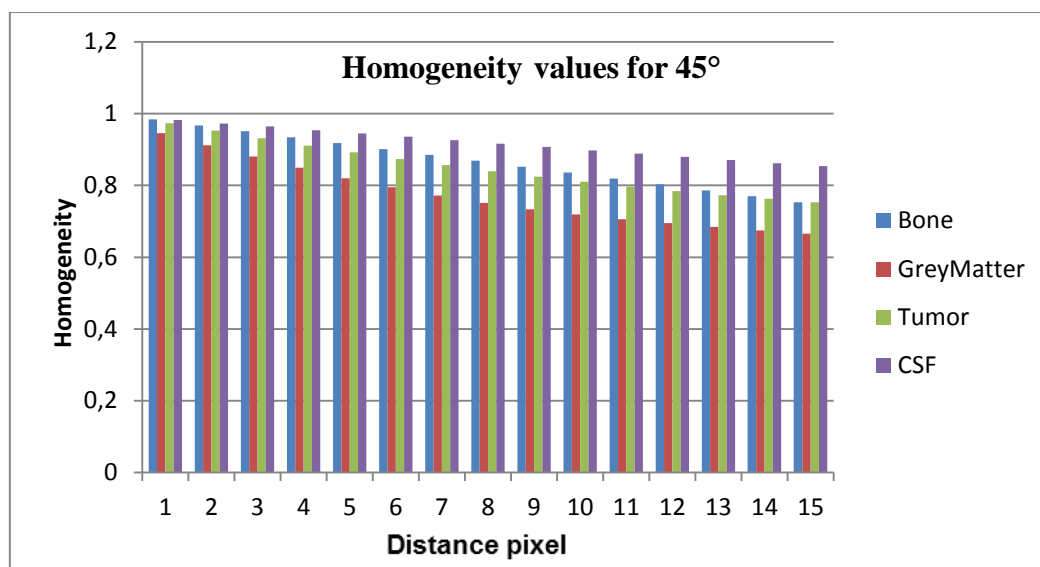


**Figure IV.6:** Contrast values for different samples (Bone, GreyMatter, Tumor, CSF) with  $\theta=135^\circ$

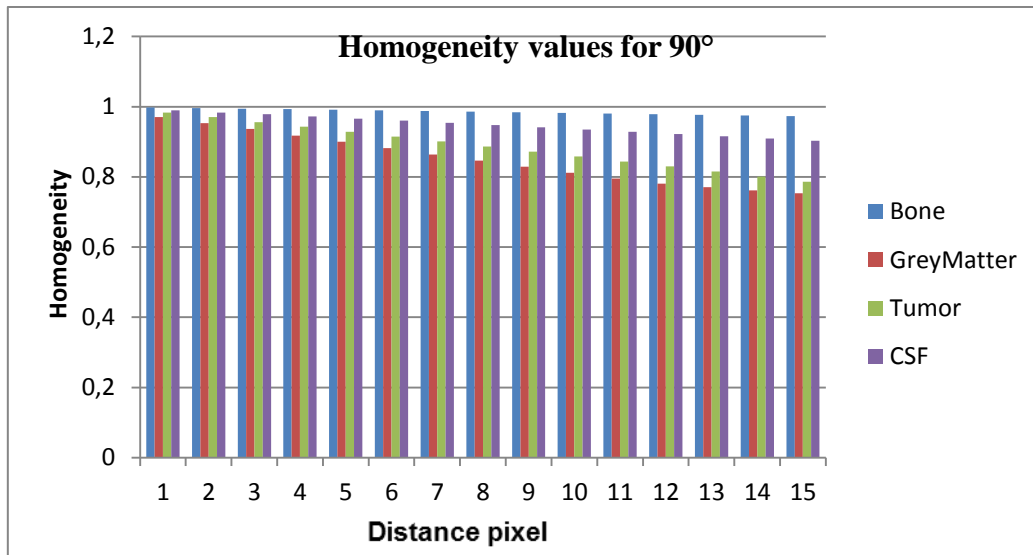
According to the above results we can clearly see that the abnormal tissue has higher contrast since there is no big difference in the grey level on the other hand for the bone since we included some undesired pixels we see that it has the lowest contrast even if it should not be the case, therefore we can consider the contrast as a parameter for the tumor characterization.



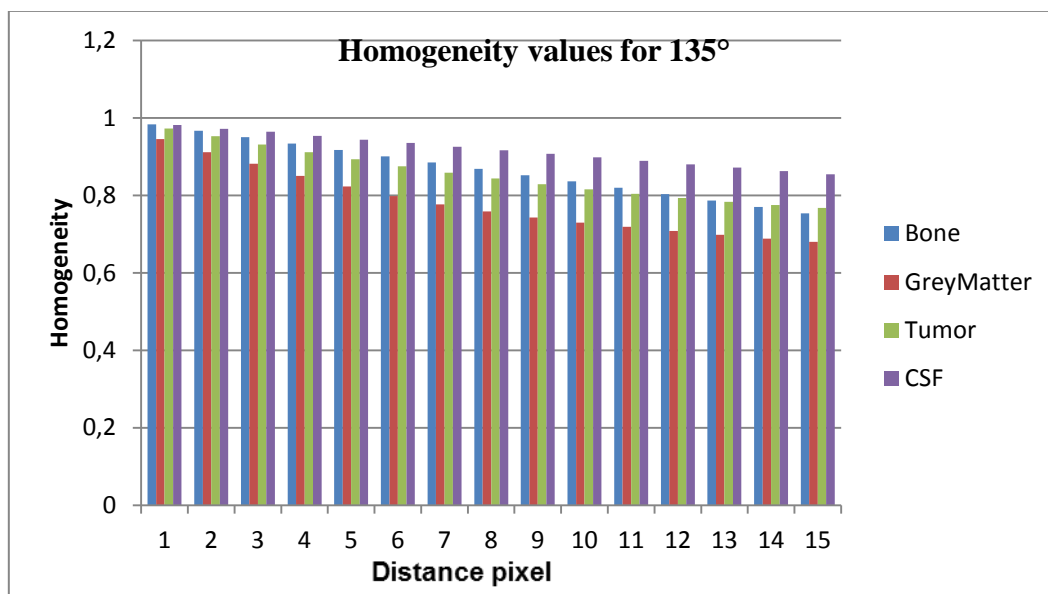
**Figure IV.7:** Homogeneity values for different samples (Bone, GreyMatter, Tumor, CSF) with  $\theta=0^\circ$



**Figure IV.8:** Homogeneity values for different samples (Bone, GreyMatter, Tumor, CSF) with  $\theta=45^\circ$

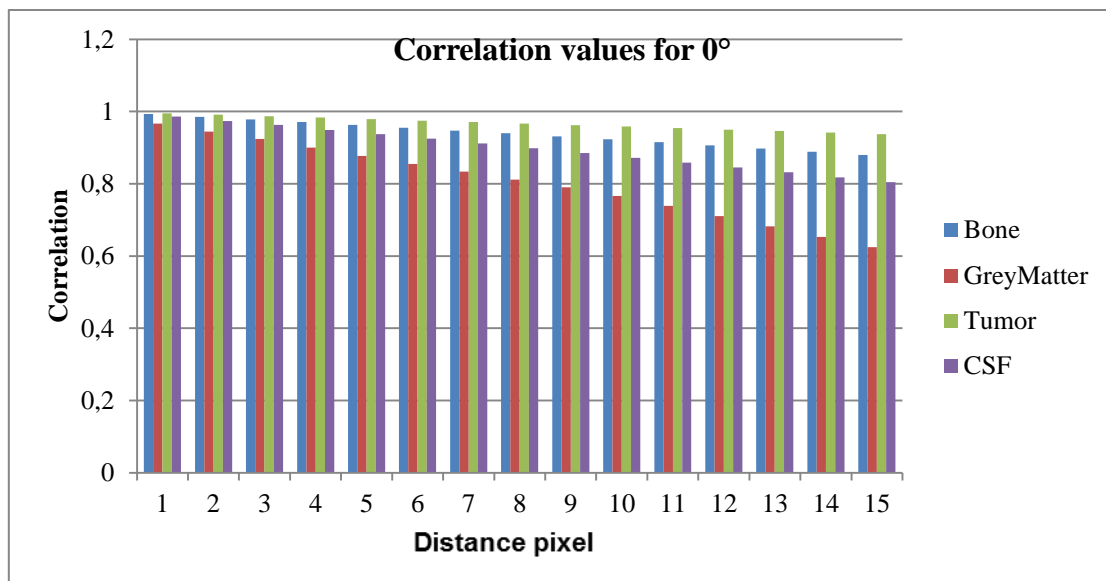


**Figure IV.9:** Homogeneity values for different samples (Bone, GreyMatter, Tumor, CSF)with  $\theta=90^\circ$

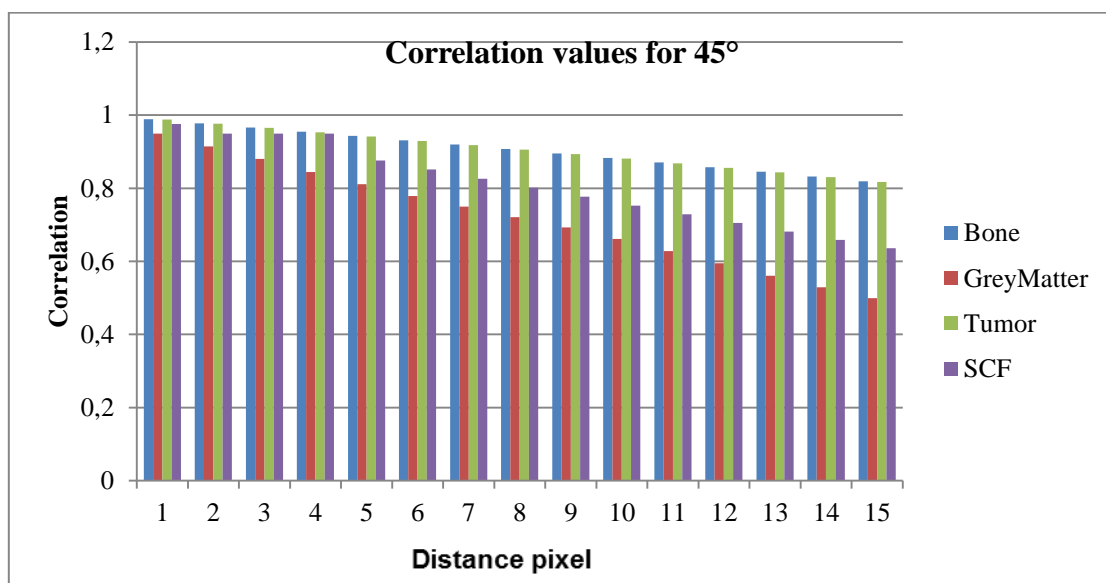


**Figure IV.10:** Homogeneity values for different samples(Bone,GreyMatter,Tumor, CSF)with  $\theta =135^\circ$

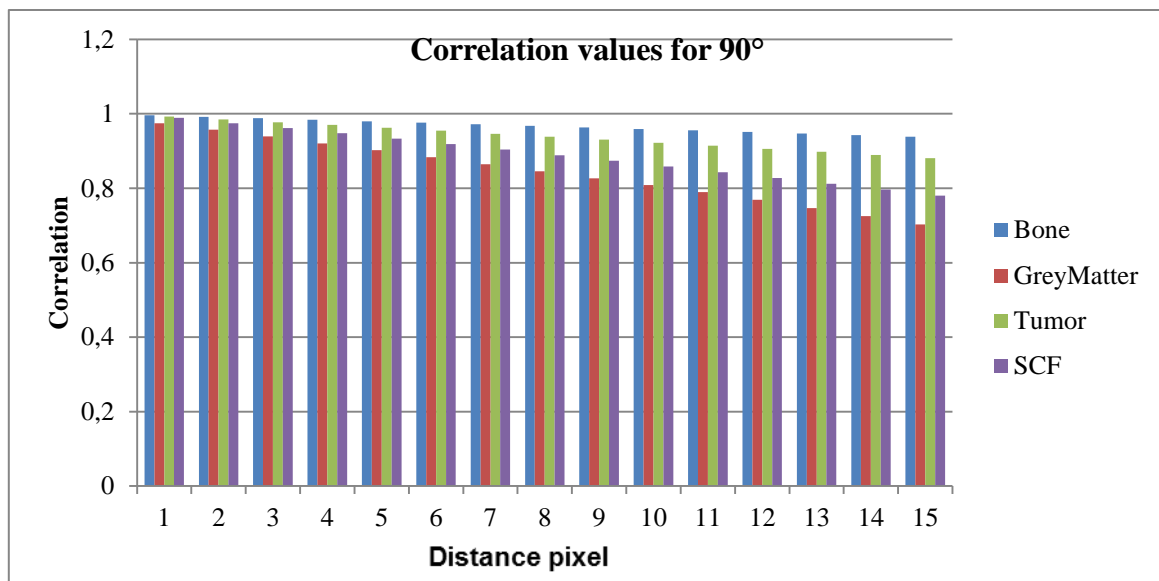
The graphs above show that there is not a big changing in homogeneity while varying the offset.



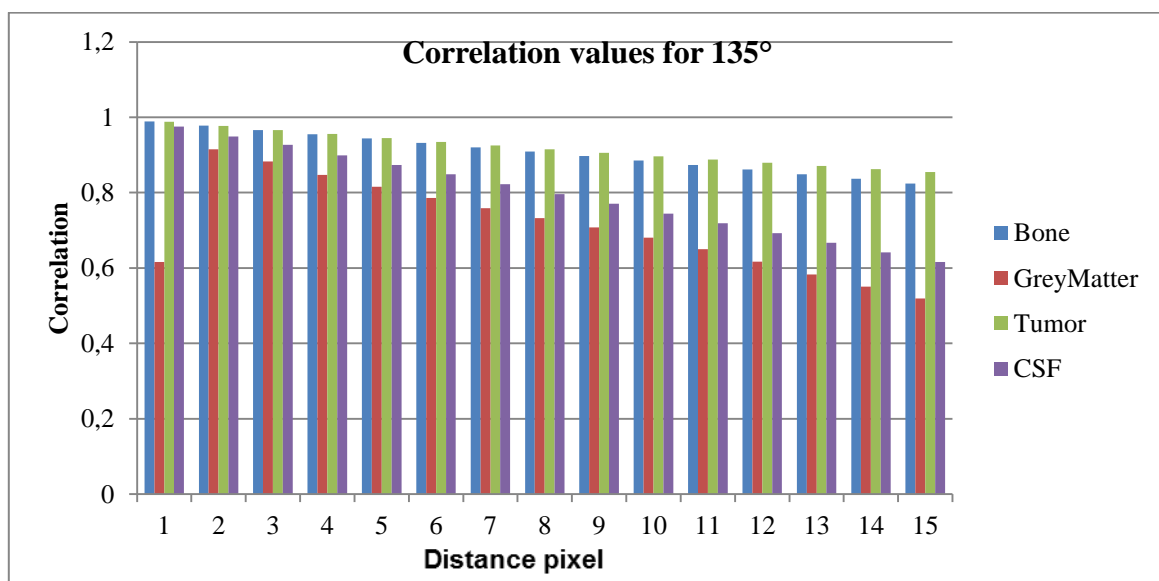
**Figure IV.11:** Correlation values for different samples (Bone, GreyMatter, Tumor, CSF) with  $\theta=0^\circ$



**Figure IV.12:** Correlation values for different samples (Bone, GreyMatter, Tumor, CSF) with  $\theta=45^\circ$

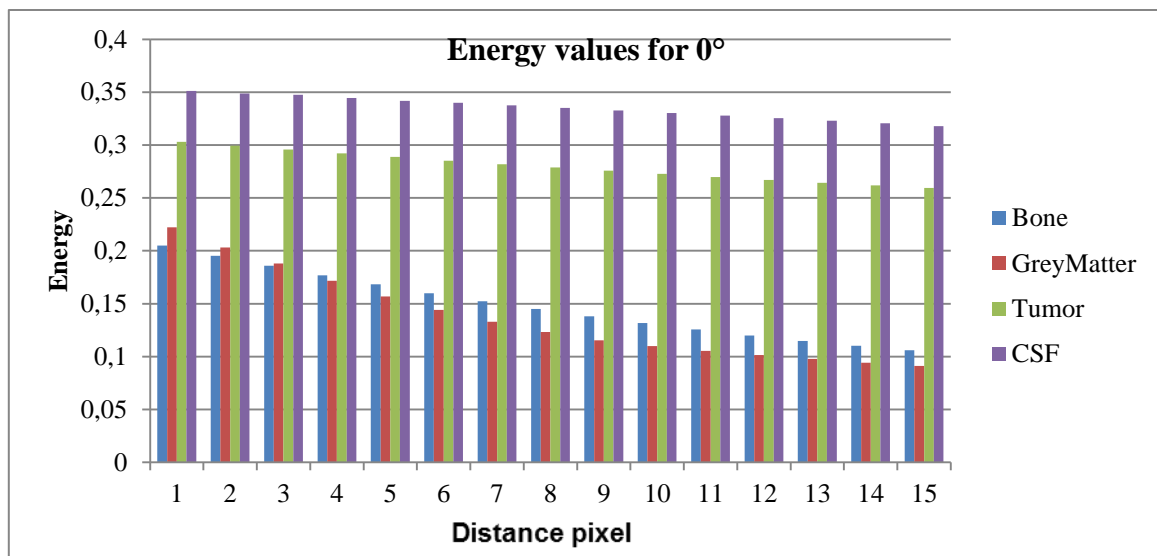


**Figure IV.13:** Correlation values for different samples (Bone, GreyMatter, Tumor, CSF) with  $\theta=90^\circ$

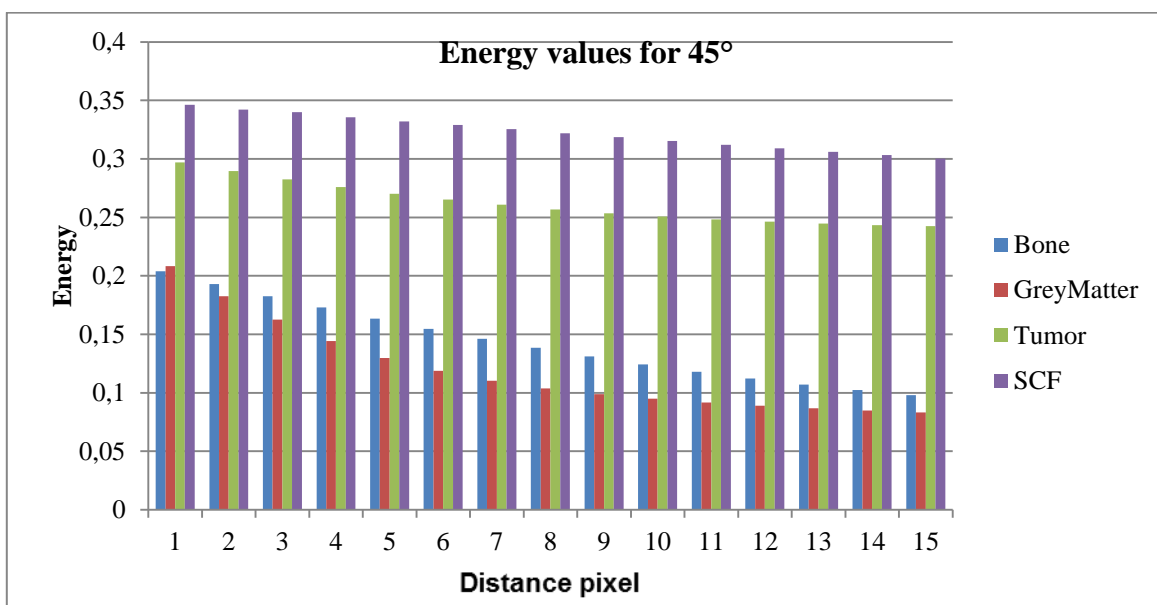


**Figure IV.14:** Correlation values for different samples (Bone, GreyMatter, Tumor, CSF) with  $\theta=135^\circ$

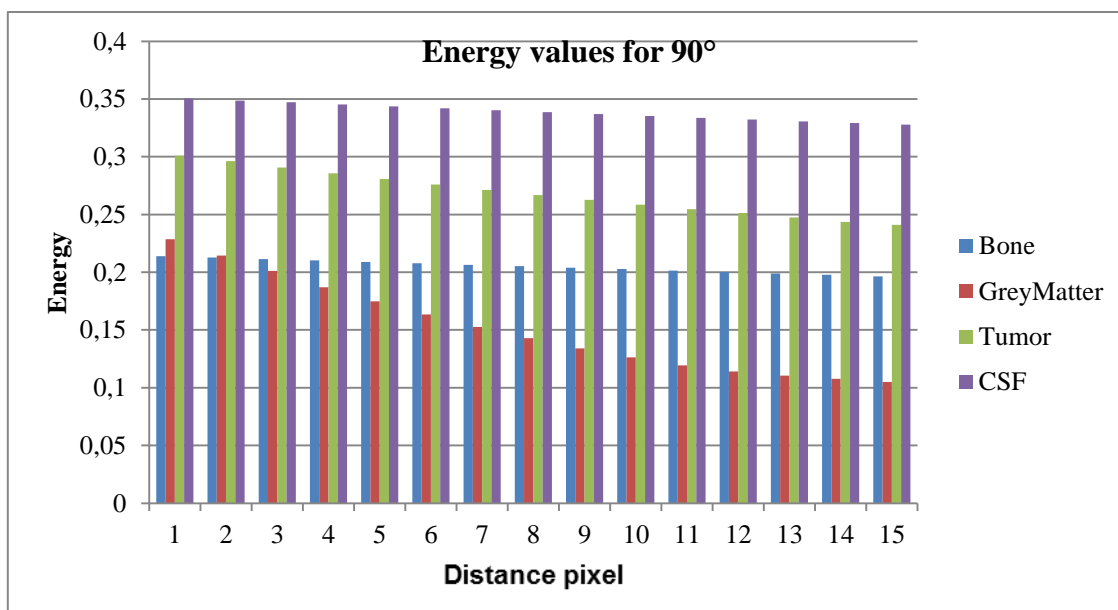
According to the graphs atop, we can see that the tumor has more correlation between the pixels which could be considered as a parameter of characterization.



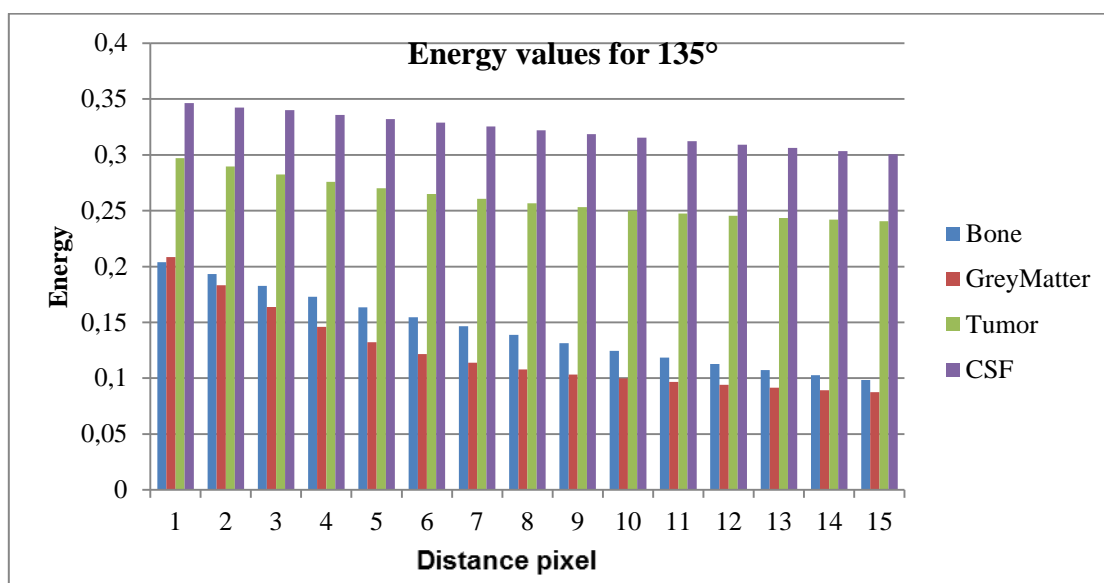
**Figure IV.15:** Energy values for different samples (Bone, GreyMatter, Tumor, CSF) with  $\theta=0^\circ$



**Figure IV.16:** Energy values for different samples (Bone, GreyMatter, Tumor, SCF) with  $\theta=45^\circ$

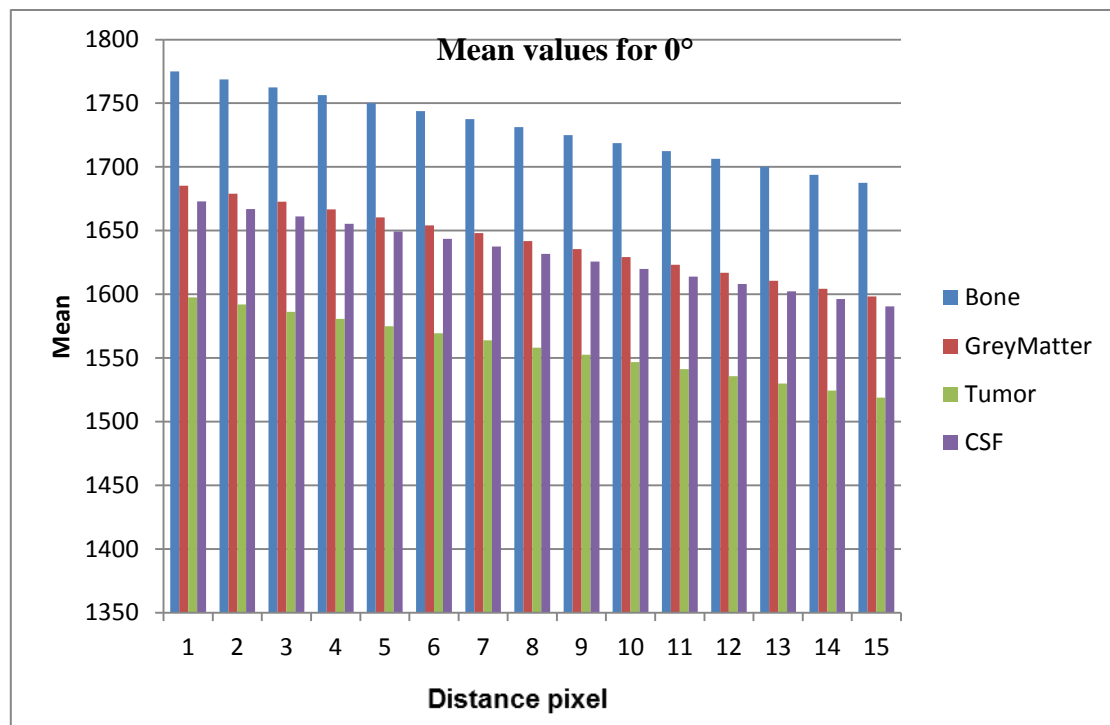


**Figure IV.17:** Energy values for different samples (Bone, GreyMatter, Tumor, CSF) with  $\theta=90^\circ$

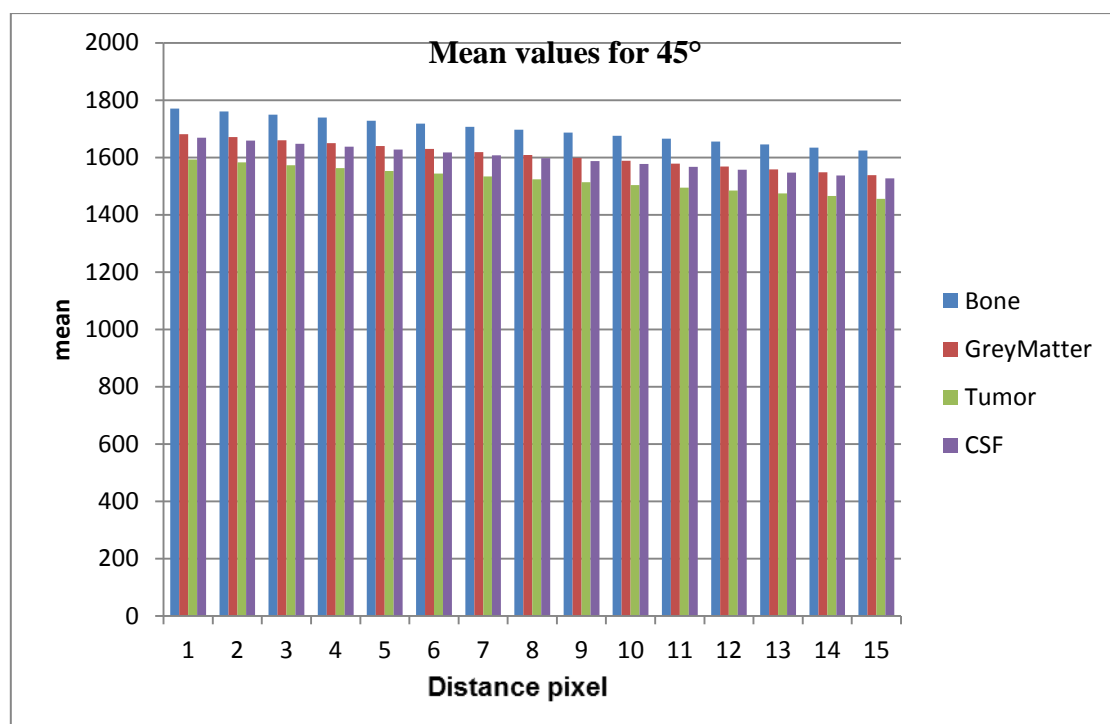


**Figure IV.18:** Energy values for different samples (Bone, GreyMatter, Tumor, CSF) with  $\theta=135^\circ$

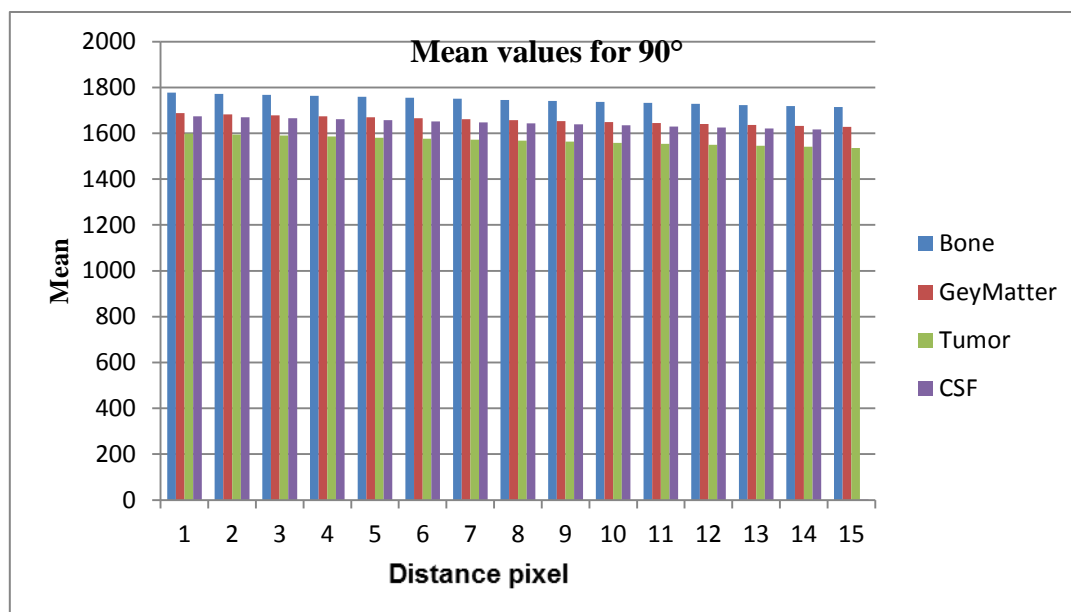
For the energy we see that the abnormal tissue (tumor) have a stable and higher energy which reflects the repetition of the pixel pairs.



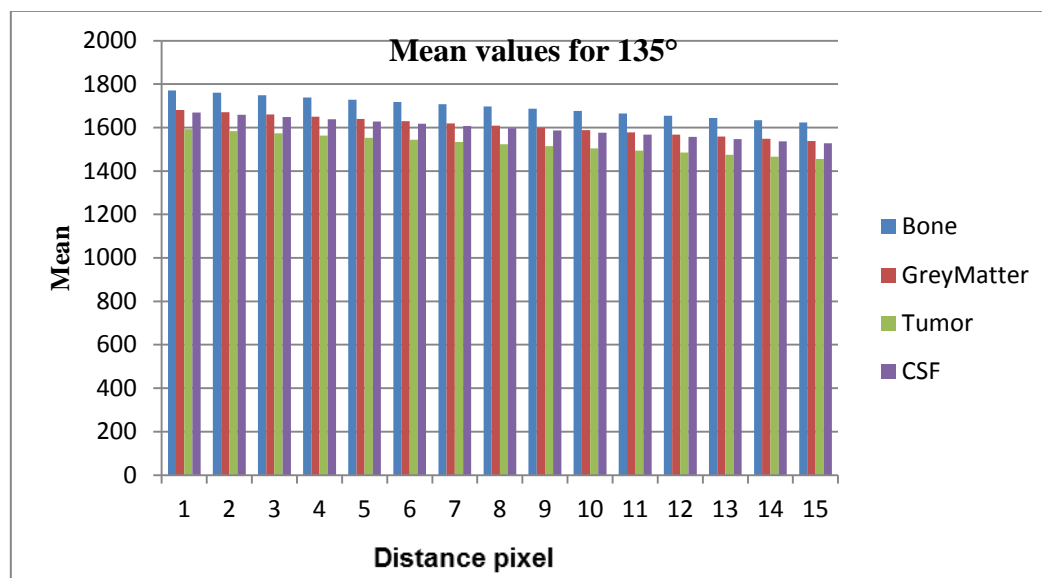
**Figure IV.19:** The mean for different samples (Bone, GreyMatter, Tumor, CSF) with  $\theta=0^\circ$



**Figure IV.20:** The mean for different samples (Bone, GreyMatter, Tumor, CSF) with  $\theta=45^\circ$



**Figure IV.21:** The mean for different samples (bone, gray matter, tumor, csf) with  $\theta=90^\circ$



**Figure IV.22:** The mean for different samples ((Bone, GreyMatter, Tumor, CSF) with  $\theta=135^\circ$

The above results show us that the abnormal tissue has lower mean rather than the normal tissues.

#### IV.4 Summary

Different MRI images have been segmented using several methods to extract the tumor, mathematical computations as well have been used for the characterization and texture analysis of different tissue, in addition to the morphological operations that have been applied for the 3D reconstruction.

# Conclusion

---

## Conclusion

In the recent clinical setting, medical imaging using MRI technique is a vital component in a great number of applications such as tumor detection which is nowadays biggest problem in healthcare sector. The ultimate challenge is to develop software with intelligence to combine imaging technology with a workable diagnostic system that is capable of detecting tumor in its early stages at that level of expert recognition of a cancer center specialist.

This work presents discussion on image segmentation that is used in image processing, after describing the medical imaging using MRI. We have developed different segmentation methods that used both region and boundary information of the image to segment the tumor; therefore, analysis and comprehensive assessment of these image segmentation techniques are done. The 3D model of the brain tumor was reconstructed from 2D slices of brain by developing methods for segmentation, inter-slice interpolation and mesh generation. The tumor was segmented before by using threshold technique. The skull part was removed. The slices with tumor were stacked. By using Marching cubes algorithm the tumor was reconstructed and different brain's part which are bone, CSF, tumor and grey matter are analyzed and characterized by calculating several texture parameters that are energy, correlation, contrast, homogeneity and the mean.

Based on this, we conclude that the proposed segmentation methods are effectively capable of identifying tumor areas. Since the KM segmentation is non deterministic algorithm, an algorithm can be proposed to minimize the time for execution. Large number of triangles are generated by the marching cubes algorithm; hence an algorithm is to be designed to minimize the triangles so that the reconstruction time speeds up.

The experimental results show that our proposed 3D reconstruction approach can generate an accurate 3D model in less time. Thus it can assist the radiologist in diagnosis, and identifying the tumor stage. Finally the texture analysis shown the difference between each part, and it gave satisfactory results in the classification of different objects composing the image.

There are a number of pathological features which contribute in determination of the tumor whether it is benign or malignant, since it is very difficult to classify it. Further, in future we would work on implementing the software to detect tumors in other parts of the body like lungs, and breast and we would calculate their volume. This will be the topic for our future research.

## References

---

### References

- [1] Ayesha Khalid Khan, Gulistan Raja and Ahmad Khalil Khan, "*Implementation of Marker based Watershed Image Segmentation on Magnetic Resonance Imaging*", Life Science Journal vol. 10, N°2, pp 115-118 ,2013;.
- [2] K. Narayan and Y. Karunakar, "*3-D Reconstruction of Tumors in MRI Images*", International Journal of Research and Reviews in Signal Acquisition and Processing, vol. 2, N°1, 2011.
- [3] N. Archip, R. Rohling, V. Dessenne, P. J. Erard and L. P. Nolte, "*Anatomical structure modeling from medical images*", Computer Methods and Programs in Biomedicine, vol. 82, pp. 203-215, 2006.
- [4] J. D. Foley, A. Van Dam, S. K..Feiner and J. F. Hughes, "*Computer graphics: principles and practice*", 2nd Edition, Addison-Wesley, Boston, 1996.
- [5]William Henry Nailon, "*Texture Analysis Methods for Medical Image Characterisation*", book chapter from Biomedical Imaging, Youxin Mao (Ed.), ISBN: 978-953-307-071-1, 2010.